



RESEARCH ARTICLE

Immunohistochemical characterization of bipolar cells in four distantly related avian species

Vaishnavi Balaji¹ | Silke Haverkamp² | Pranav Kumar Seth¹  | Anja Günther^{1,2}  |
 Ezequiel Mendoza³  | Jessica Schmidt¹  | Maike Herrmann¹ |
 Leonie Lovis Pfeiffer¹ | Pavel Němec⁴  | Constance Scharff³  |
 Henrik Mouritsen^{1,5}  | Karin Dedek^{1,5} 

¹Animal Navigation/Neurosensorics Group, Institute for Biology and Environmental Sciences, University of Oldenburg, Oldenburg, Germany

²Department Computational Neuroethology, Max Planck Institute for Neurobiology of Behavior - caesar, Bonn, Germany

³Institut für Biologie, Freie Universität Berlin, Berlin, Germany

⁴Department of Zoology, Charles University, Prague, Czech Republic

⁵Research Center Neurosensory Science, University of Oldenburg, Oldenburg, Germany

Correspondence

Karin Dedek, Animal Navigation/Neurosensorics Group, Institute for Biology and Environmental Sciences, University of Oldenburg, Oldenburg, Germany.
 Email: karin.dedek@uol.de

Funding information

Max Planck Society; Stiftung Center of Advanced European Studies and Research; Czech Science Foundation, Grant/Award Number: 22-35153S; European Research Council, Grant/Award Number: 810002; Presidential Board of the University of Oldenburg; Deutsche Forschungsgemeinschaft, Grant/Award Number: SFB1372,395940726;RTG1885/2

Abstract

Visual (and probably also magnetic) signal processing starts at the first synapse, at which photoreceptors contact different types of bipolar cells, thereby feeding information into different processing channels. In the chicken retina, 15 and 22 different bipolar cell types have been identified based on serial electron microscopy and single-cell transcriptomics, respectively. However, immunohistochemical markers for avian bipolar cells were only anecdotally described so far. Here, we systematically tested 12 antibodies for their ability to label individual bipolar cells in the bird retina and compared the eight most suitable antibodies across distantly related species, namely domestic chicken, domestic pigeon, common buzzard, and European robin, and across retinal regions. While two markers (GNB3 and EGFR) labeled specifically ON bipolar cells, most markers labeled in addition to bipolar cells also other cell types in the avian retina. Staining pattern of four markers (CD15, PKC α , PKC β , secretagoin) was species-specific. Two markers (calbindin and secretagoin) showed a different expression pattern in central and peripheral retina. For the chicken and European robin, we found slightly more ON bipolar cell somata in the inner nuclear layer than OFF bipolar cell somata. In contrast, OFF bipolar cells made more ribbon synapses than ON bipolar cells in the inner plexiform layer of these species. Finally, we also analyzed the photoreceptor connectivity of selected bipolar cell types in the European robin retina. In summary, we provide a catalog of bipolar cell markers for different bird species, which will greatly facilitate analyzing the retinal circuitry of birds on a larger scale.

KEYWORDS

AAV virus, bipolar cell, buzzard (*Buteo buteo*), chicken (*Gallus gallus*), double cone, European robin (*Erithacus rubecula*), magnetoreception, pigeon (*Columba livia*), retina

Vaishnavi Balaji, Silke Haverkamp, and Karin Dedek contributed equally.

This is an open access article under the terms of the [Creative Commons Attribution-NonCommercial](https://creativecommons.org/licenses/by-nc/4.0/) License, which permits use, distribution and reproduction in any medium, provided the original work is properly cited and is not used for commercial purposes.

© 2022 The Authors. *The Journal of Comparative Neurology* published by Wiley Periodicals LLC.

1 | INTRODUCTION

In the vertebrate retina, bipolar cells are the only interneurons that project from the outer to the inner retina. They receive and filter the information from photoreceptors and transmit it to amacrine and ganglion cells via many parallel pathways which differ in morphology and physiology (reviewed in Euler et al., 2014). Bipolar cells possess a dendritic tree making either selective (Behrens et al., 2016; Breuninger et al., 2011; Günther et al., 2021; Haverkamp et al., 2005) or nonselective photoreceptor contacts (Behrens et al., 2016; Günther et al., 2021), a soma located in the distal part of the inner nuclear layer (INL), and an axon terminal stratifying in one (e.g., mouse bipolar cells, Wässle et al., 2009) or more strata (many fish, turtle, and bird bipolar cells; Ammermüller and Kolb, 1995; Günther et al., 2021; Li et al., 2012) of the inner plexiform layer (IPL). Functionally, bipolar cells differ in their light responses: ON bipolar cells respond with a depolarization to light ON and OFF bipolar cells with a depolarization to light OFF. Some additional ON–OFF bipolar cells with color-opponent center responses (e.g. red-ON, green/blue-OFF) have been recorded in turtle and fish retina (Ammermüller et al., 1995; Wong & Dowling, 2005) and were also suggested to be present in the bird retina (Yamagata et al., 2021). In addition to response polarity, bipolar cells also differ in response transience (DeVries, 2000; Franke et al., 2017; Ichinose & Hellmer, 2016), ion channel expression (Hellmer et al., 2016; Ivanova & Müller, 2006; Puller et al., 2013), and gap junctional coupling (Fournel et al., 2021).

Bipolar cells are best studied in the mouse retina and over decades, many different techniques were used, such as immunolabeling for marker proteins (e.g., Haverkamp et al., 2003a), transgenic mouse lines (e.g., Wässle et al., 2009), cell filling (Ghosh et al., 2004; Pignatelli & Strettoi, 2004), serial electron microscopy (EM) reconstructions (Helmstaedter et al., 2013), population imaging of glutamate release (Franke et al., 2017), and single-cell transcriptomics (Shekhar et al., 2016), to classify cells. Together, these studies reached the consensus of 14 different bipolar cells (or 15, if the dendritic tree-less GluMi cell is also counted, see Della Santina et al., 2016) in the mouse retina. In birds, however, much less is known about the different bipolar cell types. In the 1980s, two studies described some bipolar cell types by Golgi staining of individual cells (pigeon: Mariani, 1987; chicken: Quesada et al., 1988). Recently, 22 different bipolar cell types were identified in chicken, based on single-cell transcriptomics (Yamagata et al., 2021). In a serial EM study, we provided a bipolar cell classification of the chicken retina (Günther et al., 2021) and described 15 different bipolar cell types, based on morphological parameters and photoreceptor connectivity. However, due to the limited depth of the EM stack, it seems likely that bipolar cells with large dendritic trees (Quesada et al., 1988) were missed in our study. To potentially find these and compare bipolar cell types across different bird species and different retinal regions, immunohistochemical markers are needed. For the bird retina, GNB3 and Islet-1 have been described as markers for ON bipolar cells (Ritchev et al., 2010) and PKC α was suggested to label rod-contacting bipolar cells in the chicken retina (Caminos et al., 1999).

Yet, a systematic screen for bipolar cell markers is missing for any bird species.

Here, we tested 12 antibodies and identified eight antibodies suitable for labeling bipolar cells in four avian species. We investigated the domestic chicken (*Gallus gallus domesticus*), the domestic pigeon (*Columba livia domestica*), which is a good homer, the common buzzard (*Buteo buteo*) as raptor with exceptional visual acuity, and the European robin (*Erithacus rubecula*) as insect-hunting night-migratory songbird (for phylogenetic relationships, see Figure 1a and b). Some markers labeled similar types of bipolar cells in all species whereas others labeled different cell types. One of the four species, the European robin, is also well known for its ability to orient with the help of the Earth's magnetic field (Mouritsen, 2018; Wiltschko & Wiltschko, 1972; Zapka et al., 2009) during nighttime migration. This ability is based on a light-dependent process (Hore & Mouritsen, 2016; Ritz et al., 2000; Xu et al., 2021), which seems to start in the retina (Heyers et al., 2007; Liedvogel et al., 2007; Mouritsen et al., 2005), namely in the double cone photoreceptors (Chetverikova et al., 2022; Günther et al., 2018). To gain more insights into the retinal downstream circuitry that might be involved in magnetoreception, we also studied the photoreceptor connectivity of selected bipolar cell types in the European robin retina.

2 | METHODS

2.1 | Experimental animals and tissue preparation

In this study, we used the retinæ from three domestic chickens, eight European robins, two domestic pigeons, and three buzzards. Chickens and pigeons were bred and raised in the animal facility of University of Oldenburg (Lower Saxony, Germany). Six European robins were caught with mist nets in the vicinity of the Oldenburg University campus. Bird catching was done based on a permit from the Lower Saxony State Department for Waterway, Coastal and Nature Conservation (NLWKN, D7.2220/18). Chickens (aged between 2 and 4 weeks), pigeons (aged > 2 months), and robins (adult) were dark adapted for at least 1 h before sacrifice. European robins were sacrificed by decapitation, domestic chickens were sacrificed by decapitation if they weighed less than 250 g; otherwise, they were sacrificed prior to decapitation by an overdose of Narcoren, as were the pigeons. All animal procedures were performed in accordance with local, national, and EU guidelines for the use of animals in research and were approved by the Animal Care and Use Committees of the *Niedersächsisches Landesamt für Verbraucherschutz und Lebensmittelsicherheit* (LAVES, Oldenburg, Germany).

For immunohistochemistry, eyes were quickly removed from the orbits and the anterior part of the eye was cut with a razor blade and separated from the rest of the eyecup. Eyecups were immediately transferred into 4% paraformaldehyde (PFA, prepared in 0.1 M phosphate-buffered saline, PBS) for 30 min. After 2–3 washes in PBS for 30 min, eyecups were subsequently immersed in 10% and 20% sucrose in PBS for 40–60 min each and then in 30% sucrose overnight.

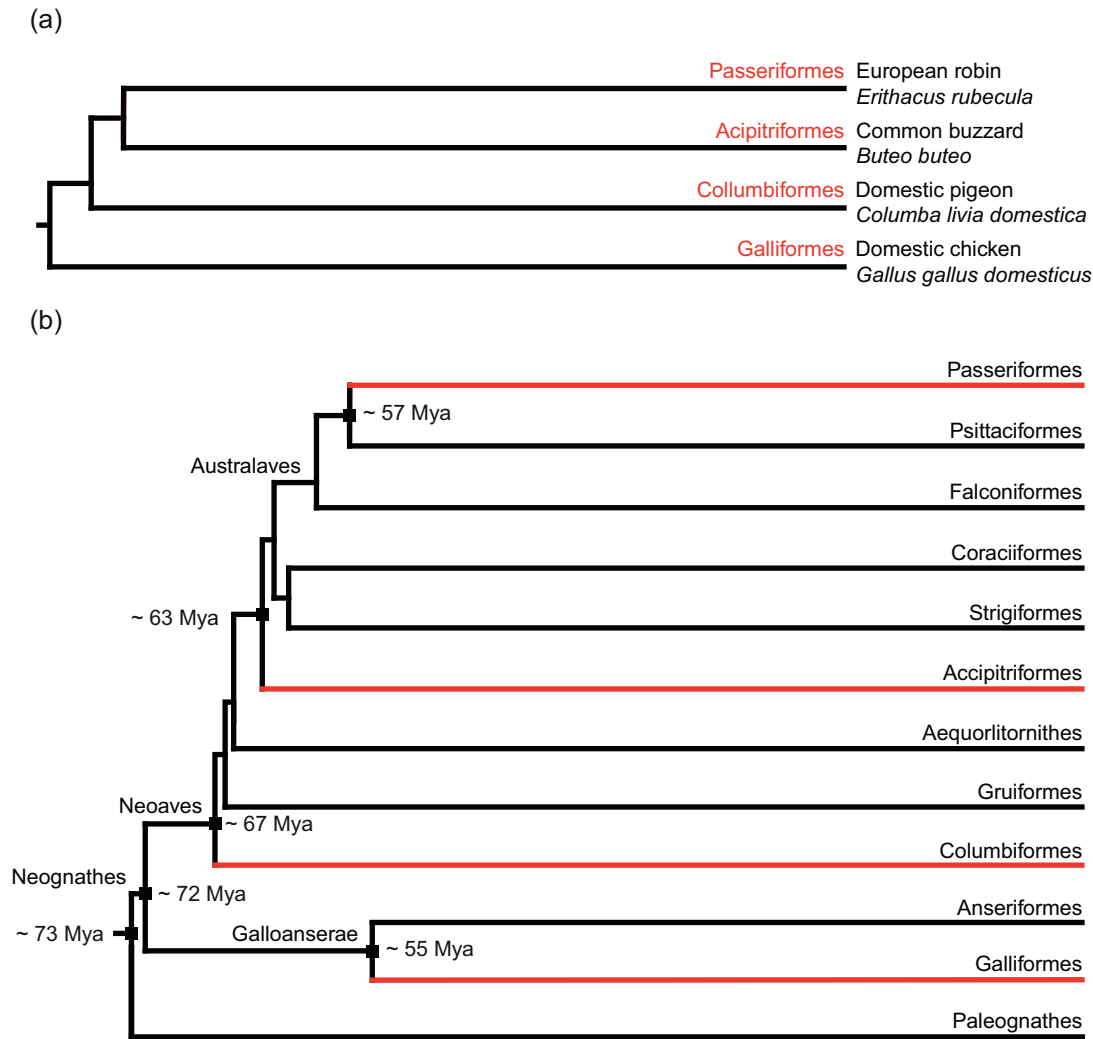


FIGURE 1 Phylogenetic trees, highlighting the species investigated. Phylogenetic relationships between the four species examined (a) and their phylogenetic position within major avian clades (b). The topology and branch lengths of the time-calibrated tree follows the study by Prum et al. (2015). Mya, million years ago

All eyecups were preserved in 30% sucrose in PBS and stored at -20°C until further use for cryosectioning.

Two European robins were caught with mist nets in the vicinity of Prague. Buzzards were injured animals with a low probability of recovery obtained from animal rescue centers in the Czech Republic. The eyes became available when the animals were killed for a study of their brains (Kverková et al., 2022). The animals received a lethal dose of halothane and were then transcardially perfused with heparinized, warmed phosphate-buffered saline (pH 7.4) followed by cold phosphate-buffered 4% paraformaldehyde solution. All procedures were approved by Institutional Animal Care and Use Committee at Charles University in Prague and Ministry of Culture of the Czech Republic (permission number UKPRF/28830/2021). The eyes were dissected, postfixed by immersion for 1 h in the same fixative, rinsed in PB, incubated in 30% sucrose solution for 24 h, transferred into antifreeze (30% glycerol, 30% ethylene glycol, 40% phosphate buffer) and frozen for further processing.

2.2 | Antibody characterization

Table 1 lists all antibodies used in this study and their sources.

The polyclonal calbindin (Calb) antibody from guinea pig recognizes human calbindin D28k and produces a band of 28 kDa in a western blot from rat brain homogenate. It labeled the same cells in the bird retina as a polyclonal calbindin antibody raised in rabbit which we used earlier (Haverkamp et al., 2021).

The mouse anti-calsenilin antibody recognizes a specific band in western blot analysis of mouse retina extracts. After blocking with GST-calsenilin, immunoreactivity is absent (Haverkamp et al., 2008).

Antibodies against the carbohydrate epitope CD15 (cluster of differentiation 15) label flat (OFF) midget bipolar cells in marmoset. This staining pattern has been well established in a previous study (Haverkamp et al., 2021).

The antibody directed against C-terminal binding protein 2 (Ctbp2) was tested on retina homogenates and recognized a double band of

TABLE 1 Primary antibodies used in this study

Antibody	Antigen	Host & type	Dilution	Source, cat#, RRID
Calbindin	Calbindin D-28k	Guinea pig	1:1000	Synaptic Systems, 214005, RRID:AB_2619902
Calsenilin	Synthetic peptide directed towards the N-terminal region of human CSEN	Rabbit polyclonal	1:500	Aviva Systems Biology, ARP31932_P050, RRID:AB_389152
CD15	U-937 histiocytic cell line	Mouse monoclonal	1:100	BD Biosciences, 559045 RRID:AB_397181
Ctbp2	Synthetic peptide corresponding to aa 974–988 from rat Ribeye	Rabbit polyclonal	1:1000	Synaptic System, 193 003 RRID: AB_2086768
EGF	The immunogen is a green fluorescent protein (GFP) fusion protein corresponding to the full length amino acid sequence (246 aa) derived from the jellyfish <i>Aequorea victoria</i>	Goat Polyclonal	1:500	Rockland, 600-101-215, RRID:AB_218182
EGFR	Raised against recombinant protein corresponding to aa 1019–1168 of human EGFR's cytoplasmic domain	Rabbit polyclonal	1:100–500	Novus Biologicals, NBP1-84814, RRID:AB_11016401
GNB3	Peptide with sequence SGHDNRVSLGVT, corresponding to aa 309–321 of human transducin β chain 3	Goat polyclonal	1:200	Aviva Systems Biology, OALA06860, RRID:AB_2909439
HCN1	Fusion protein aa 778–910 of rat HCN1 (cytoplasmic C-terminus), clone N70/28	Mouse monoclonal	1:500	NeuroMab, 75-110, RRID:AB_2115181
HCN4	GST fusion protein with a sequence corresponding to aa 119–155 of human HCN4	Rabbit polyclonal	1:500	Alomone Labs, APC-052, RRID:AB_2039906
Islet1	<i>E. coli</i> -derived recombinant human Islet-1 (aa 4–349)	Goat polyclonal	1:250	R&D Systems AF1837, RRID:AB_2126324
Islet1	C-terminal of recombinant rat Islet-1 (aa 178–349)	Mouse monoclonal	1:50	DSHB, 40.2D6, RRID:AB_528315, developed by Jessell, T.M./Brenner-Morton, S.
Pax6	Recombinant partial protein (N-terminal region, aa 1–223 of chicken Pax6)	Mouse monoclonal	1:50	DSHB, Pax6, RRID:AB_528427, developed by Kawakami, A.
PKARII β	Human protein kinase A, regulatory subunit II β (aa 1–418)	Mouse monoclonal	1:2000	BD Biosciences Cat# 610625, RRID:AB_397957
PKC α	Hinge region (aa 292–317) of protein kinase	Mouse monoclonal	1:500	Santa Cruz Biotechnology, sc-80, RRID:AB_628141
PKC β	Epitope mapping between aa 656–671 at the C-terminus of PKC β 1 of human origin	Mouse monoclonal	1:100	Santa Cruz Biotechnology, sc-8049, RRID:AB_628143
PSD95	Recombinant protein corresponding to aa 68–251 from mouse PSD95	Rabbit Polyclonal	1:1000	Synaptic Systems, 124 008, RRID:AB_2832231
Recoverin	Recombinant human recoverin	Rabbit polyclonal	1:1000	Millipore, AB5585, RRID:AB_2253622
SCGN	Recombinant human secretagoin with N-terminal His tag	Sheep polyclonal	1:200	BioVendor, RD184120100, RRID:AB_2034060

aa, amino acids.

ribeye (the retina-specific variant of Ctbp2). Also, it detected an over-expressed EGFP-Ctbp2 fusion construct but showed no cross-reaction with EGFP-Ctbp1 (Hübler et al., 2012). In bird retina, it was already used successfully to label ribbon synapses (Günther et al., 2021).

According to the manufacturer, the antibody directed against the enhanced green fluorescent protein (EGFP) was prepared from antiserum by immunoaffinity chromatography using GFP coupled to agarose beads followed by solid phase adsorption(s) to remove any unwanted reactivities. Assay by immunoelectrophoresis resulted in a single precipitin arc against anti-goat serum and purified and partially purified GFP. No reaction was observed against human, mouse or rat serum proteins.

According to the manufacturer, the antibody against epidermal growth factor (EGFR) shows a band of the correct size (~175 kDa) in western blots of a rat cell line. Staining in human placenta was strong but absent from tonsil tissue, as expected from RNAseq data for the same tissues.

The antibody against GNB3 (G-protein subunit β 3) recognizes human GNB3 and GNB4. On avian tissue this antibody gave a similar staining as a rabbit GNB3 antibody described earlier (Ritchev et al., 2010).

The monoclonal HCN1 antibody directed against the hyperpolarization- and cyclic nucleotide-gated channel (HCN) 1 recognizes a single band of 100 kDa in western blots of mouse brain membrane, according to the manufacturer. This band is absent in HCN1 knockout mice. The antibody does not cross-react with HCN2.

The HCN4 antibody was identified as a marker for type 3a mouse bipolar cells. Western blot and immunohistochemical staining results are the same as for several independent HCN4 antibodies (Mataruga et al., 2007; Wässle et al., 2009).

The 40.2D6 monoclonal antibody recognizes both Islet1 and Islet2. Its staining pattern closely resembles the human Islet1 antibody (see below) and is well described in the chicken retina (Fischer et al., 2008).

According to the manufacturer, the antibody against human Islet1 was controlled by western blot and immunocytochemistry. It recognized a single band of ~42 kDa in lysates of human induced pluripotent stem cells differentiated into motoneurons.

The Pax6 antibody was developed by Dr. A. Kawakami (Division of Biological Science, University of Tokyo, Japan). The staining described here reproduces earlier results from chicken retina (Fischer et al., 2007).

The antibody directed against protein kinase A, regulatory subunit II β (PKARII β) labels a subtype of mouse bipolar cells (type 3b). On western blots with retinal tissue, it detects a single band of 53 kDa as in human endothelial cells, which served as positive control (Mataruga et al., 2007).

Antibodies against the α subunit of protein kinase C (PKC α) recognize a single band of the appropriate size (80 kDa) in western blot experiments with Jurkat cells. Its staining on avian tissue resembles the staining earlier reported for the chicken retina (Caminos et al., 1999).

According to the manufacturer, the antibody against human PKC β 1 was controlled by western blot and immunocytochemistry. It recognizes a single band of ~87 kDa in mouse brain tissue extract.

According to the manufacturer, the PSD95 (postsynaptic density protein 95) antibody has been verified on knockout tissue. Staining results (see below) showed a similar pattern in the bird retina as described earlier for the mammalian retina (Koulen et al., 1998).

The antibody against recoverin recognizes a single band of 26 kDa on western blots of human retina and detected bipolar cells in different species (Haverkamp et al., 2003a; Puller et al., 2011).

The sheep anti-secretogin (SCGN) antibody recognizes a single band of the predicted size (~32 kDa) on western blots of mouse retinal lysates (Puthussery et al., 2010).

2.3 | Virus production

The virus used in the experiments is an AAV serotype 2/9, containing a CAG promoter driving the expression of EGFP. To generate the virus, the ArchT-tdTomato sequence was cut out of the plasmid pAAV-CAG-ArchT-tdTomato (Addgene plasmid #29778; <http://n2t.net/addgene:29778>; RRID:Addgene_29778; gift from Edward Boyden) with the restriction enzymes BamHI and EcoRI. The resulting construct was used as the backbone into which EGFP was cloned. The virus was produced and its titer quantified via genomic qPCR by the Viral Core Facility of Charité—Universitätsmedizin Berlin, Germany. The titer of the virus was 3.97×10^{12} vg/ml.

2.4 | Intravitreal injections

Adeno-associated viruses (AAV2/9-CAG-eGFP) containing the coding sequence of EGFP were intravitreally injected into the left eyes of two European robins. Injections were performed based on a permit from LAVES (33.9-42502-04-17/2566). As preventive measures against vomiting and pain, robins were food-deprived for 2 h and injected with 50 μ l of meloxicam (0.2 mg/kg) intramuscularly, respectively, prior to the surgery and gently wrapped in a bandage to restrict wing motion and keep the birds stable during the injection procedure. Birds were anaesthetized with isoflurane (2% initially and then 1.5%–1.7% throughout the surgery) and their breathing rate was observed until it got stable (48 breaths/min). The eye lid was pulled back carefully using a hooked suture. Using a 27G needle, a hole was punctured at the sclera-cornea junction and a 33G Hamilton needle containing the injection solution was inserted. Approximately 10 μ l of the AAV diluted in PBS were injected into the left eye. The right eye was not injected. After the injection, the needle was left in the eye for ~10 s to prevent reflux of the viral suspension out of the eye. Finally, the suture was cut and the bandage removed. The bird was kept on a warming plate to recover from anesthesia before it was returned to a cage. Virus-injected birds were regularly monitored for their health and behavior and sacrificed 25 and 180 days after injection.

2.5 | Immunostainings

For chicken, robin, and pigeon retina, vertical sections (20 μ m thick) were cut on a cryostat, dried on a hot plate for at least 45 min, and

stored at -20°C . For buzzard and occasionally robin retina, vertical sections ($100\ \mu\text{m}$) were cut with a vibratome (Leica VT 1200 S). Slices were washed three times for 10 min in PBS and then blocked with 5% donkey and/or goat serum and 0.3% TritonX-100 in PBS for 1 h. For stainings with SCGN, the blocking step was omitted. Primary antibodies (Table 1) were applied in blocking solution overnight at 4°C . On the next day, slices were washed several times in PBS and then incubated with secondary antibodies (diluted in blocking solution) for 2 h at room temperature. Donkey secondary antibodies were conjugated to Alexa 488 or Alexa 568 (dilution 1:500, Thermo Fisher Scientific, Waltham, MA, USA) or to Alexa 647 (dilution 1:250, Thermo Fisher Scientific; Dianova, Hamburg, Germany). After several washing steps, slices were mounted in Aqua-Poly/Mount or Vectashield with DAPI. The specificity of the secondary antibodies was tested by incubation without primary antibodies. No unspecific staining was detected.

2.6 | Microscopy and image analysis

Images were acquired with a confocal laser scanning microscope (Leica TCS SP8), using an HC PL APO 40x/1.3 or HC PL APO 63x/1.4 oil immersion objective. The voxel size was adjusted with respect to the experimental question. During data analyses with Fiji (Schindelin et al., 2012), the background was adjusted using the *Subtract Background* function and intensities were normalized using the *Contrast Enhancement* function with 0–0.4 saturation. Unless stated otherwise, sum or maximum projections of confocal stacks are shown (thickness 0.4–1 μm , 2–5 optical sections). Images were occasionally filtered for presentation purposes.

The *Cell counter* plugin in Fiji was used to count the number of (a) ON versus OFF bipolar cells in regions of interest covering the bipolar cells in the inner nuclear layer (INL) and (b) ribbon synapses of ON versus OFF bipolar cells in regions of interest covering the entire inner plexiform layer (IPL). Ribbon counts are based on substacks with 3–4 optical scans (0.2 μm), nuclei counts are based on ~ 20 optical scans (0.25 μm).

3 | RESULTS

Earlier studies suggest the presence of 10–22 different bipolar cell types in chicken (Günther et al., 2021; Quesada et al., 1988; Yamagata et al., 2021) and pigeon retina (Mariani, 1987). Here, we searched for markers labeling individual types of bipolar cells in distantly related avian species (Figure 1a and b), using domestic chicken, pigeon, European robin, and common buzzard as models.

Antibodies were chosen based on previous studies, with a focus on antibodies that are (1) commercially available, (2) do not label all bipolar cells (thereby excluding for example Otx2, Yamagata et al., 2021), and (3) were shown to label bipolar cells in mammalian species.

First, we double-labeled retinæ for GNB3 and Islet1 to test whether these markers label ON bipolar cells (as reported for the chicken: Ritchey et al., 2010) in all investigated species. However, for the buzzard retina, we show both markers (raised in goat) as single staining because the mouse monoclonal Islet1 antibody did not

work in combination with GNB3. Consistent with previous reports (Haverkamp et al., 2021; Ritchey et al., 2010), Islet1 labeled the cell nuclei of putative horizontal cells, bipolar cells, starburst amacrine cells, and ganglion cells in all four bird species (Stanke et al., 2008; Haverkamp et al., 2021; Figure 2a–d). However, we found notable differences in the distribution of Islet1+ bipolar cells in the INL. In chicken and pigeon (Figure 2a and b), Islet1+ bipolar cells occurred close to the horizontal cells, uniformly covering largely the distal half of the INL. In contrast, Islet1+ bipolar cells seemed organized in three layers in the INL in the European robin (Figure 2c): a distal layer with weakly Islet1+ nuclei (1), a middle (2) and a proximal layer (3, close to amacrine cell bodies), with more brightly labeled nuclei.

When applied together (Figure 2a–c), Islet1 and GNB3 antibodies labeled the same cells within one species, with Islet1 labeling nuclei and GNB3 staining cell membranes, confirming that Islet1 and GNB3 are expressed in the same cell type (i.e., the ON bipolar cells) in the bird retina. Thereby, GNB3 staining clearly revealed the stratification pattern of ON bipolar cells in the inner plexiform layer (IPL). In all species investigated (Figure 2a–d), the distal half of the IPL hardly contained GNB3+ terminals, whereas the proximal half showed several prominent GNB3+ bands, interspersed with GNB3– bands. This suggests that avian ON bipolar cells stratify predominantly in the proximal half of the IPL whereas OFF bipolar cells stratify mostly in the distal half but additionally in the proximal “ON layer,” as was suggested before (Figure 2c, Günther et al., 2021).

We also counted the number of ribbon synapses belonging to ON and OFF bipolar cell terminals. For this purpose, we labeled the peripheral chicken (recounted from the stack available in Extended Data Figure 6–1 in Günther et al., 2021) and peripheral European robin retina for Ctbp2 to label all bipolar cell ribbons and GNB3 to label all ON bipolar cell terminals. Consequently, Ctbp2+/GNB3+ ribbons were counted as ON and Ctbp2+/GNB3– ribbons were counted as OFF bipolar cell synapses. OFF bipolar cell ribbons outnumbered ON bipolar cell ribbons by a factor of 1.2 in the chicken (OFF: 393 ± 16 ribbons/50 μm IPL; ON: 333 ± 22 ribbons/50 μm IPL; counts from four substacks in one retina) and 1.3 in the European robin (OFF: 721 ± 244 ribbons/50 μm IPL; ON: 560 ± 152 ribbons/50 μm IPL; counts from eight substacks from two retinæ from two different animals). Whether this OFF:ON ratio is similar in the central retina is hard to resolve because ribbons are so numerous in the European robin retina that we could not count them reliably in central regions.

As the distribution of ON and OFF bipolar cell somata seemed to differ between different bird species (see above), we additionally estimated the relative number of ON versus OFF bipolar cells in the central INL of the chicken and the European robin. For this purpose, we used triple labeling with Pax6 (labeling all horizontal and amacrine cells; Fischer et al., 2007; Yamagata et al., 2021), Islet1 (Fischer et al., 2007), and DAPI (labeling all nuclei). DAPI+ but Islet1–/Pax6– cells were counted as OFF bipolar cells, DAPI+/Islet1+/Pax6– cells were counted as ON bipolar cells. In both species, ON bipolar cells slightly outnumbered OFF bipolar cells (chicken: 54% Islet1+/Pax6– ON bipolar cells, 46% Islet1–/Pax6– OFF bipolar cells; European robin: 55% versus 45%; counts from three substacks in one retina each). Together, this data suggests that there are slightly more ON bipolar cells than OFF

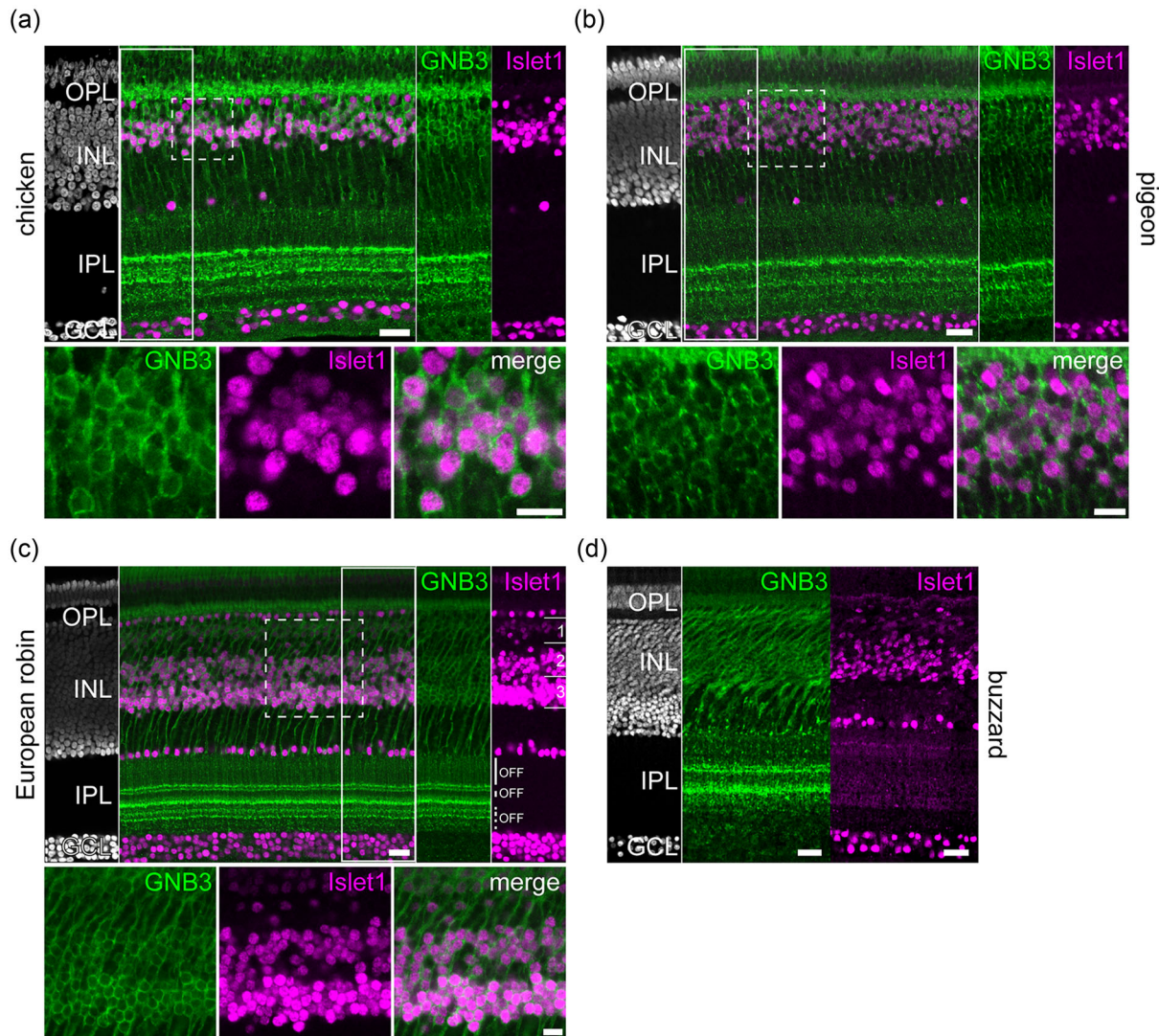


FIGURE 2 Distribution of GNB3+ and Islet1+ ON bipolar cells in different avian species. Labeling for GNB3 and Islet1 in the central chicken (a), pigeon (b), and European robin retina (c). As Islet1 antibodies did not work in the buzzard retina in combination with GNB3, both markers are shown separately (d). Areas marked by boxes in (a–c) are shown as single channel images next to the overlay (solid white line) and as magnifications below the overlay (dashed white line). DAPI labeled sections on the left (gray) serve to reveal all cell nuclei and retina layers. Among others, Islet1 labeled the nuclei of ON bipolar cells, whereas GNB3 stained the membranes of ON bipolar cells, visualizing the many different strata in the avian inner plexiform layer (IPL). Putative OFF layers, also present in the presumed ON layers, are labeled exemplarily in (c) with white bars. In the European robin, Islet+ bipolar cells form three layers which are marked in the single scan for Islet1 in (c). Note that Islet1 staining intensities were saturated on purpose to reveal the weakly labeled ON bipolar cell nuclei in the distal inner nuclear layer (INL). GCL, ganglion cell layer; OPL, outer plexiform layer. Scale: 20 μm

bipolar cells in the bird INL and slightly more OFF bipolar cell ribbons than ON bipolar cells ribbons in its IPL.

3.1 | Bipolar cell markers tested on four different avian species

To screen for markers that label individual types of bipolar cells in the avian retina, we performed immunohistochemistry with antibodies directed against PKC α and β (Figures 3 and 4), CD15 (Figure 5), HCN1 (Figure 6), EGFR (Figure 7), SCGN (Figure 8), and Calb (Figure 9). Additionally, we tested common markers for mammalian bipolar cells, such as calsenilin, HCN4, recoverin, and PKA regulatory subunit

$\text{I}\beta$ (data not shown because staining of bipolar cells was weak or absent).

Antibodies against PKC α and β are used as markers for ON bipolar cells in different vertebrate species (Günther et al., 2021; Haug et al., 2019; Haverkamp and Wässle, 2000; Haverkamp et al., 2003b; Ritchey et al., 2010). In the European robin and buzzard retina, Islet1+ ON bipolar cells were prominently labeled for PKC α (Figure 3a and b), including the axon terminals. However, Islet- OFF bipolar cells were also labeled, although weaker than ON bipolar cells in the European robin (Figure 3a and b). In European robin, also most amacrine cells were faintly outlined. Colabeling with GNB3 confirmed that PKC α labels ON bipolar cells in the European robin (Figure 4a, layers 2–5).

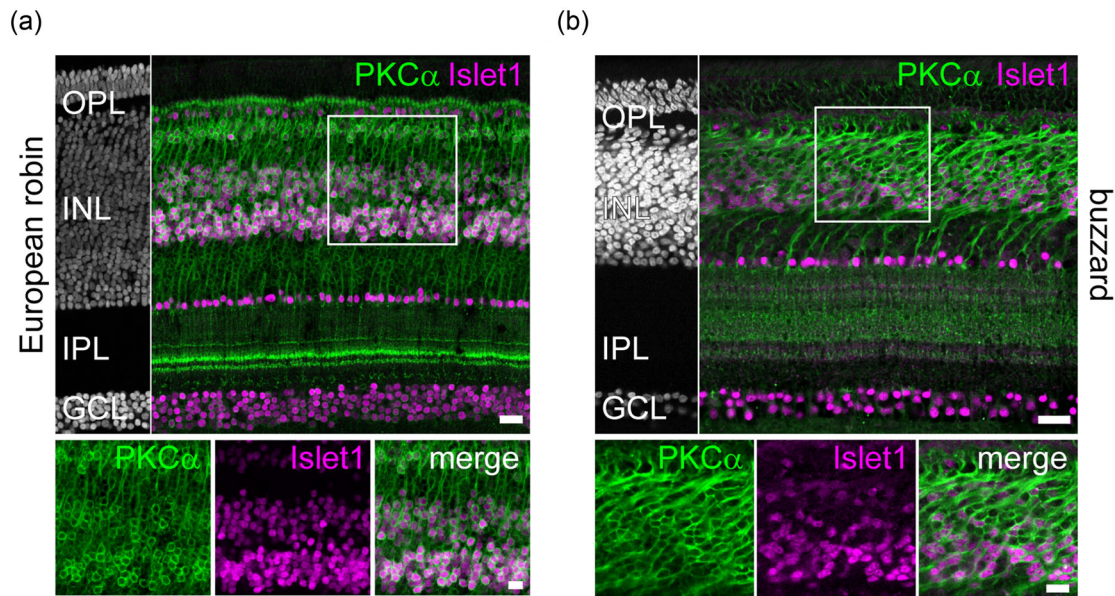


FIGURE 3 Labeling for the α subunit of protein kinase C in European robin and buzzard retina. Labeling for Islet1 and PKC α in central European robin (a) and buzzard retina (b). In both species, many bipolar cells were labeled with PKC α . DAPI labeled sections in (a, b) serve to reveal all cell nuclei and retina layers. Areas marked by the white squares are shown in higher magnification at the bottom. GCL, ganglion cell layer; INL, inner nuclear layer; OPL, outer plexiform layer. Scale: 20 μ m (top), 10 μ m (bottom)

Also, antibodies against PKC β stained GNB3+ ON bipolar cells in this species (Figure 4a). However, as GNB3 showed two additional prominent bands in the IPL (Figure 4a, layers 1 and 6), we conclude that not all ON bipolar cells are labeled by PKC α and β . Notably, PKC β antibodies also revealed distinct ganglion cells in the European robin retina (Figure 4a).

Stainings differed in the IPL of the buzzard: PKC β antibodies stained three prominent bands, one in the distal IPL (likely representing the stratification of amacrine cell dendrites, Figure 4b, arrow), and two in the proximal IPL, GNB3+ bands were less pronounced in between, and PKC α + bands covered the distal 75% of the IPL and were almost absent from the proximal 25% (Figures 3b and 4b).

Antibodies against CD15 are reported to label OFF midget and DB6 ON bipolar cells in the marmoset retina (Chan et al., 2001; Haverkamp et al., 2021). Here, we show that CD15 antibodies label different populations of bipolar cells in the four avian species we examined. In the chicken retina, double-labeling with Islet1 revealed that CD15+ bipolar cells are either Islet1+ (Figure 5a, arrowhead) or Islet1- (Figure 5a, short arrow), suggesting that CD15 labels at least two different populations of bipolar cells in this species. In contrast, CD15 antibodies exclusively labeled a population of wide-field Islet1+ ON bipolar cells in the pigeon retina (Figure 5b). This cell type contains a prominent Landolt's club in the outer nuclear layer, a cellular extension traversing from the outer plexiform to the outer nuclear layer (Figure 5b, long arrow). In the European robin, CD15+ bipolar cells comprised Islet1+ (Figure 5c, arrowheads) and Islet1- cells (Figure 5c, short arrow). Islet1- CD15+ bipolar cells had their somata close to the amacrine cells and exhibited an extremely long dendrite, terminating with a large dendritic tree (see Figure 12b) in the outer plexiform layer (OPL). In the buzzard, CD15+

bipolar cells were all Islet1- and thus represent OFF bipolar cells (Figure 5d, short arrows). Due to strong CD15 immunoreactivity in amacrine cells, the stratification of CD15+ bipolar cells in the IPL could not be discerned in any of the avian species we examined (Figure 5).

HCN1 was demonstrated to label OFF bipolar cells in the rabbit retina (Kim et al., 2003). In all four avian species, antibodies against HCN1 labeled distinct populations of bipolar cells, in addition to amacrine cells. HCN1+ bipolar cells were Islet1+ in chicken, pigeon, and European robin retina (Figure 6a–c, arrowheads). These ON bipolar cells exhibited a Landolt's club in chicken and pigeon (Figure 6a and b) and may represent wide-field ON bipolar cells in the pigeon retina (Figure 6b). In the European robin retina, cells were rather numerous with somata in the distal INL, potentially representing a single type. In buzzard, HCN1 staining was weak and could not be combined with Islet1 (Figure 6d).

EGFR antibodies exclusively labeled a subset of Islet1+ ON bipolar cells in the four avian species we investigated (Figure 7a–d, arrowheads). EGFR+ bipolar cells in the chicken retina had their somata close to the horizontal cells in the distal INL, contained a Landolt's club and showed two distinct stratification bands close to the middle of the IPL (Figure 7a). In contrast, EGFR+ ON bipolar cells (Figure 7b, arrowheads) in the pigeon retina were less ordered and did not show a Landolt's club but had a similar stratification pattern as in the chicken. EGFR staining in the European robin retina looked very similar to that in chicken. Notably, all Islet1+ bipolar cells in the distal INL were also EGFR+. Two prominent stratification bands were visible in the robin IPL (Figure 7c). In the buzzard retina, besides prominently EGFR+, Islet1+ cells (Figure 7d, arrowheads) in the distal INL, weakly labeled cells in the middle of the INL were discernible. The buzzard IPL

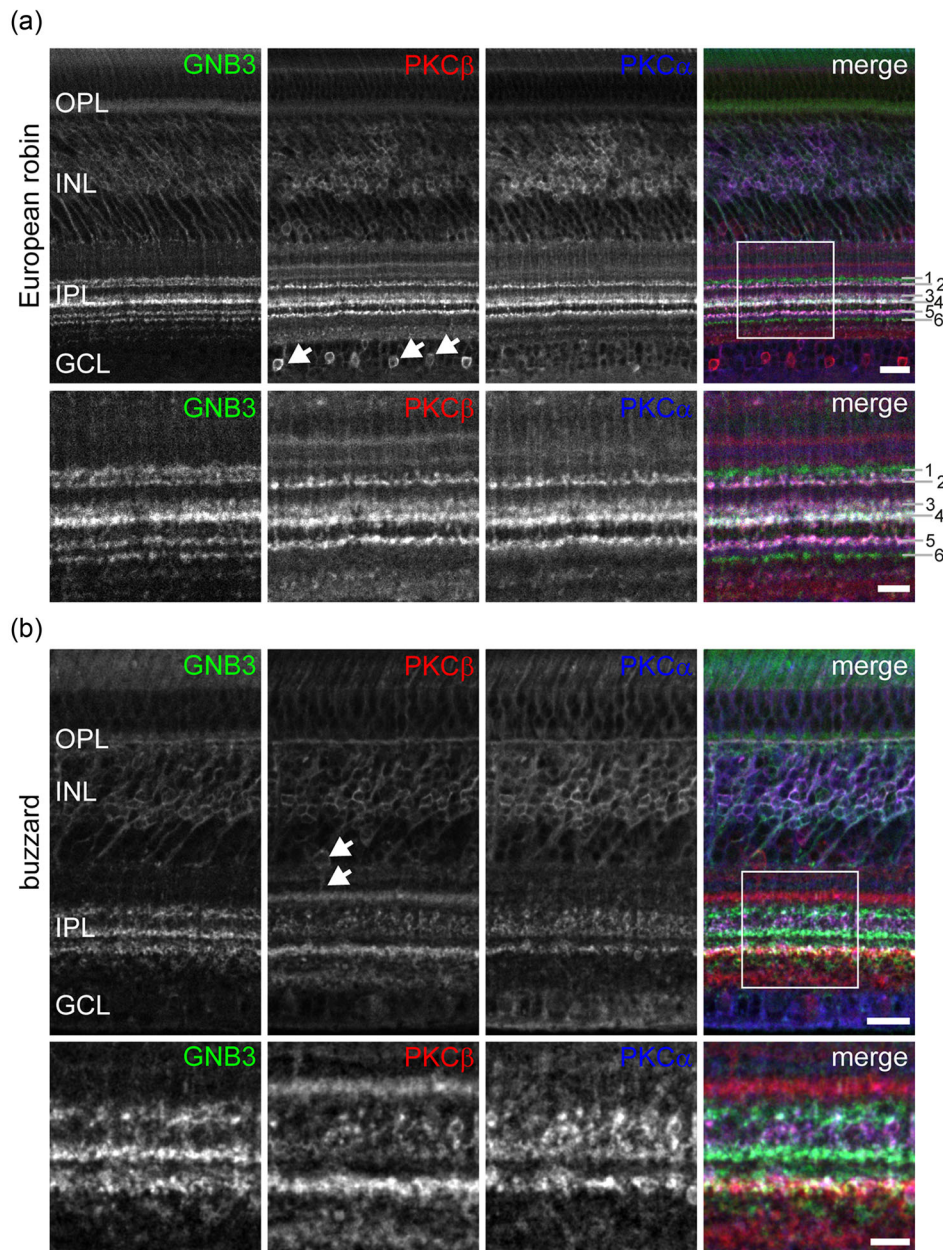


FIGURE 4 Labeling for different protein kinase C isoforms and GNB3 in European robin and buzzard retina. Labeling for GNB3, PKC α , and PKC β revealed similar pattern for PKC α and PKC β in European robin (a) but not buzzard retina (b, peripheral retina shown). Based on GNB3, PKC α and PKC β labeling, six different ON bipolar cell strata can be identified in the inner plexiform layer (IPL) of the European robin retina (a, numbers in rightmost panels, see also Figure 13). Antibodies for PKC β also labeled ganglion cells in the European robin retina (a, arrows) and amacrine cells in the buzzard retina, stratifying in the most distal PKC β + band of the IPL (b, arrows). Areas marked by the white square are shown in higher magnification. GCL, ganglion cell layer; INL, inner nuclear layer; OPL, outer plexiform layer. Scale: 20 μ m (top), 10 μ m (bottom panels)

only contained a single EGFR+ band but faintly labeled processes were visible in the proximal part of the IPL (Figure 7d).

SCGN is a Ca²⁺-binding protein with low affinity and is expressed in bipolar cells (Puthussery et al., 2010, 2011) and amacrine cells (Dudczig et al., 2017; Weltzien et al., 2014) in different species. Here, we labeled the avian retina with an antibody against SCGN and found very different staining pattern (Figure 8), depending on the species and retinal region examined. In chicken and the peripheral pigeon

retina (Figure 8a and b), the staining resembled calretinin labeling (Fischer et al., 2007; Haverkamp et al., 2021) with prominent staining of horizontal cells and some amacrine cells. Bipolar cells were only weakly SCGN+. In the central pigeon retina, some amacrine cells and somata in the ganglion cell layer (GCL) were SCGN+ but hardly any bipolar cells. A similar pattern was seen in the peripheral buzzard retina (Figure 8d). In contrast, the central European robin and buzzard retina contained many SCGN+ bipolar cells in the middle of the INL and some SCGN+

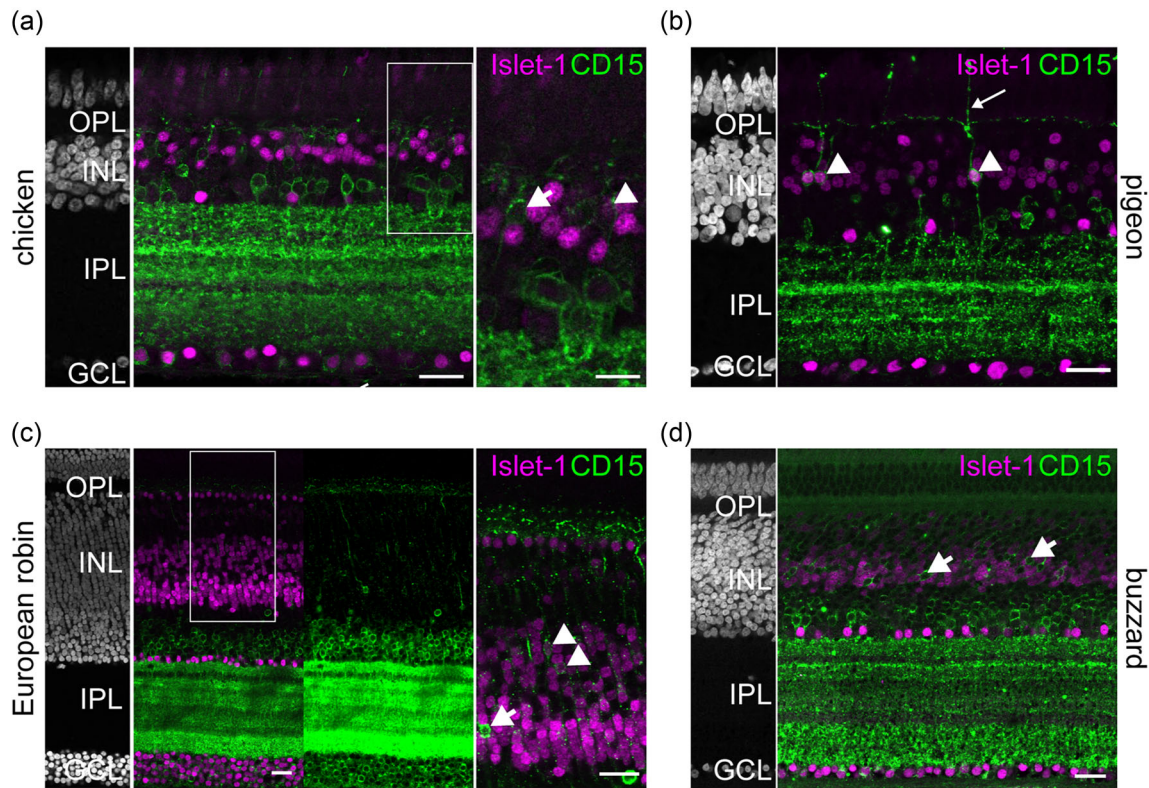


FIGURE 5 CD15 labels ON bipolar cells in pigeon, OFF bipolar cells in buzzard, and both types in chicken and European robin retina. Labeling for Islet1 and CD15 in chicken (a), pigeon (b), European robin (c) and buzzard retina (d). Areas marked by boxes in (a) and (c) are shown as single channel images on right of the overlay. CD15+ cells in the chicken were mostly Islet1- (short arrow) and occasionally Islet1+ (arrowhead). CD15+ bipolar cells in pigeon are ON cells as they were Islet1+ (arrowhead). In European robin, both ON and OFF bipolar cells were labeled, as CD15+ bipolar cells are Islet1- (short arrow) or Islet1+ (arrowhead). CD15+ cells in buzzard are OFF cells as they were Islet1- (short arrows). In pigeon (b) and European robin (c), CD15+ bipolar cells have very elaborate dendritic trees. The long arrow in (b) points to a Landolt's club. To demonstrate all cell nuclei and retina layers, we added DAPI labeled sections to the left of the stainings (a–d). Note that CD15 staining intensity in (c) was saturated on purpose to reveal the long dendrite of Islet1-/CD15+ bipolar cells reaching up to the outer plexiform layer (OPL). GCL, ganglion cell layer; INL, inner nuclear layer; IPL, inner plexiform layer. Scale: 20 μ m

amacrine cells. Clear SCGN+ stratification bands were visible throughout the European robin IPL and in the distal and proximal part of the buzzard IPL (Figure 8c and d). The SCGN+ bipolar cells in the buzzard retina were bistratified, stratifying into the most distal and the proximal band (Figure 8d, arrows).

Calbindin (Calb) represents a further Ca^{2+} binding protein, which is expressed in several different retinal cell types in chicken and pigeon retina (Fischer et al., 2007; Pasteels et al., 1990), including double cones, bipolar, horizontal, amacrine, and ganglion cells. In European robin and buzzard retina, we found—similar to SCGN—marked differences between peripheral and central retinal regions. The central retina of the European robin (Figure 9a) contained Calb+ double cones and amacrine cells and weakly labeled bipolar cells that were Islet1+ (Figure 9a, arrowheads). In the peripheral retina, the stratification pattern of these ON bipolar cells (Figure 9b, arrowheads) also became visible as two distinct bands in the middle of the IPL (Figure 9b, short arrows). In the central buzzard retina, Calb antibodies only labeled amacrine cells that stratified in a broad band in the middle of the IPL (Figure 9c). However, in the far periphery, Calb+ double cones and

bipolar cells could be discerned. These cells were also partially EGFR+ (Figure 9d, arrowheads) and stratified in two bands in the middle of the IPL, with the distal band exclusively originating from Calb+/EGFR+ bipolar cells and the proximal band originating from Calb+/EGFR- bipolar cells (Figure 9d, arrowheads) and Calb+/EGFR- bipolar cells (Figure 9d, arrow).

In summary, we identified several markers for avian bipolar cells of which HCN1 and Calb seemed specific for an individual cell type. The other markers labeled at least two different types of bipolar cells (e.g., EGFR) and often differed in their staining pattern between the avian species examined here (summarized in Table 2).

3.2 | Bipolar cells of the European robin retina

The retina of the European robin is of particular interest because it is very likely that it does not only transduce light into electrical signals but also magnetic stimuli (see Introduction; Hore and Mouritsen, 2016). As magnetic signals are presumably transmitted from photoreceptors

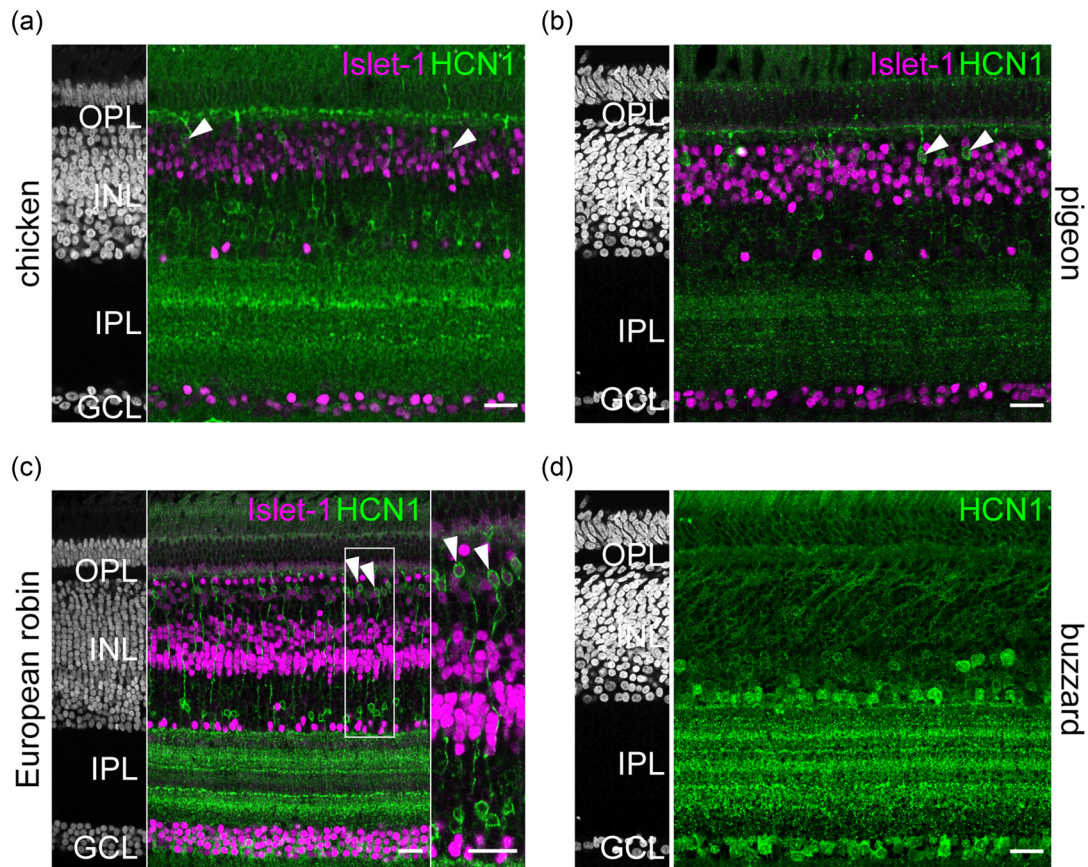


FIGURE 6 HCN1 is a marker for a distinct population of ON bipolar cells in some avian species. Labeling for Islet1 and hyperpolarization- and cyclic nucleotide-gated channel 1 (HCN1) in chicken (a), pigeon (b), and European robin retina (c) revealed that HCN1 labels Islet1+ ON bipolar cells (arrowheads) and some amacrine cells. For buzzard, only HCN1 is shown (d), which labeled bipolar cells and, more prominently, many amacrine cells. DAPI labeled sections on the left side of the immunostainings serve to reveal all cell nuclei and retina layers (a-d). GCL, ganglion cell layer; INL, inner nuclear layer; IPL, inner plexiform layer; OPL, outer plexiform layer. Scale: 20 μ m

TABLE 2 Summary of markers

Labeling/species	Chicken	Pigeon	European robin	Buzzard
GNB3	ON BC	ON BC	ON BC	ON BC
Islet1	ON BC, HC, SAC, RGC	ON BC, HC, SAC, RGC	ON BC, HC, SAC, RGC	ON BC, HC, SAC, RGC
PKC α	ON BC (Caminos et al., 1999)	n.d.	ON BC (strongly labeled), OFF BC, AC (both weakly labeled)	ON + OFF BC, AC*
PKC β	n.d.	n.d.	ON BC, AC, RGC	ON BC, AC
CD15	AC, ON BC, OFF BC	AC, ON BC	AC, ON BC, OFF BC	AC, OFF BC
HCN1	ON BC, AC	ON BC, AC	ON BC, AC	BC, AC, RGC
EGFR	ON BC	ON BC	ON BC	ON BC
SCGN	PR, HC, AC, RGC	HC, ** BC, ** AC, RGC	BC	BC, AC, ** RGC*
Calb	PR, HC, AC, RGC (Rogers, 1989)	PR, HC, AC, RGC (Pasteels et al., 1990)	PR, HC, ** ON BC, ** AC	PR, ** AC, ON BC**

AC, amacrine cells; BC, bipolar cells; HC, horizontal cells; PR, photoreceptor; RGC, retinal ganglion cells; SAC, starburst amacrine cells; n.d., not determined.

*Only in central retina.

**Only in peripheral retina.

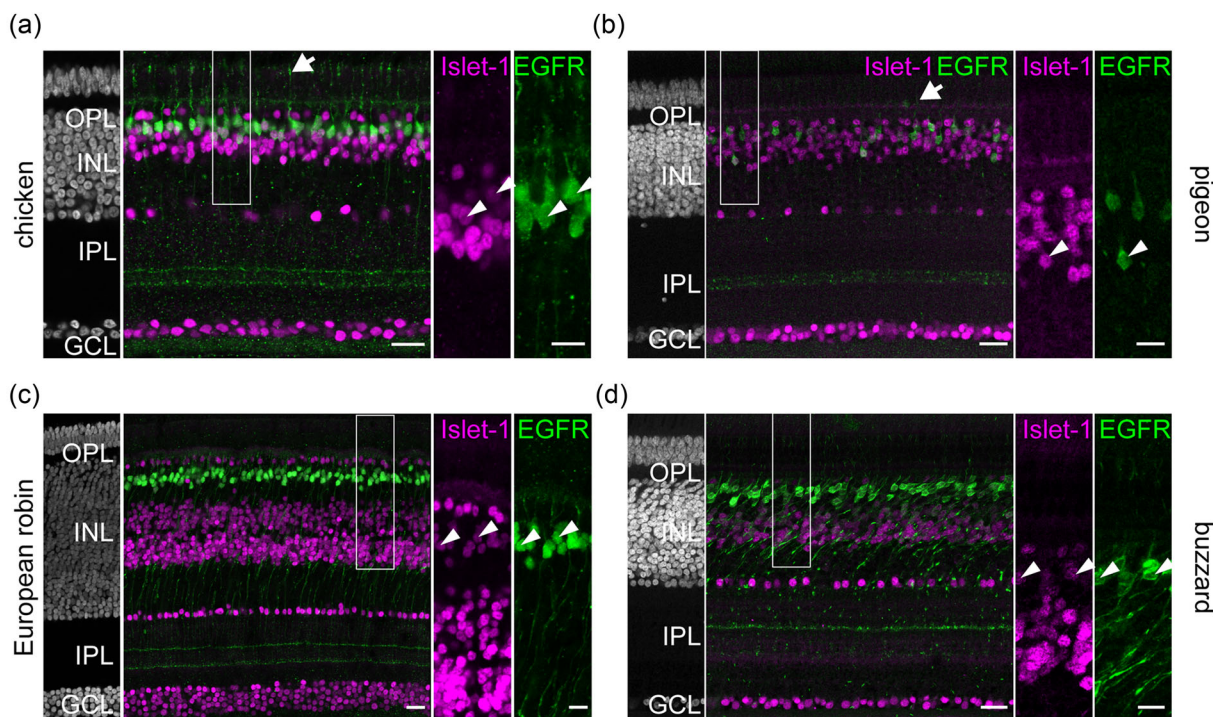


FIGURE 7 EGFR is a marker for distinct types of ON bipolar cells in different avian species. Labeling for Islet1 and epidermal growth factor receptor (EGFR) in chicken (a), pigeon (b), European robin retina (c) and buzzard retina (d). This marker seems to label similar ON bipolar cell types (Islet1+, arrowheads) in all investigated bird species. Areas marked by boxes in (a–d) are shown as single channel images next to the overlay. No other cell class is EGFR+, which allows to discern the stratification of EGFR+ bipolar cells in the inner plexiform layer (IPL). Colabeling with HCN1 shows at least for the European robin retina, that EGFR+ ON bipolar cells comprise two types (EGFR+/HCN1- and EGFR+/HCN1+, see Figure 10c). Landolt's clubs are clearly visible for EGFR+ ON bipolar cells in the chicken retina (a, arrow), but only faintly in pigeon retina (b, arrow). DAPI labeled sections next to the immunostainings serve to reveal the cell nuclei and retina layers (a–d). Areas marked with boxes are shown in higher magnification at the right side of the overlay. GCL, ganglion cell layer; INL, inner nuclear layer; OPL, outer plexiform layer. Scale: 20 μ m

to bipolar cells, we combined the different bipolar cell markers we identified to characterize the European robin retina more specifically.

Double-labeling for EGFR and PKC α revealed that EGFR+ bipolar cells are a subset of PKC α + bipolar cells. They constitute the most distal PKC α + band in the IPL and contribute to the third PKC α + band in the IPL (Figure 10a, arrowheads). Some of the PKC α + /EGFR+ ON bipolar cells are most likely also HCN1+: the combination of HCN1 with GNB3 (Figure 10b) revealed that the second most distal GNB3 band coincides with HCN1 and this band was PKC α + (please compare Figure 4a and Figure 10b, arrowheads). Combining EGFR and HCN1 antibodies confirmed that HCN1+ ON bipolar cells represent a subset of EGFR+ ON bipolar cells in the European robin retina (Figure 10c, arrowheads). In contrast, triple labeling for CD15, EGFR, and SCGN showed that these antibodies label separate populations of bipolar cells in the European robin (Figure 10d).

3.3 | Photoreceptor/bipolar cell contacts in the European robin retina

As magnetoreception may be initiated in the photoreceptors of the European robin retina (Chetverikova et al., 2022; Günther et al., 2018),

we analyzed the connections between photoreceptors and bipolar cells. We used HCN1, PKC α , and CD15 as markers for bipolar cells because these markers showed a defined staining pattern in the OPL and allowed discerning bipolar cell dendrites. Entire photoreceptors were labeled by intravitreal AAV injection, which led to the expression of EGFP in various types of photoreceptors; additionally, we used PSD95 to label all photoreceptor terminals. Photoreceptor types were identified by their morphology and stratification pattern in the OPL as double cones and rods stratify in the most distal, green, and red cones in the middle and UV and blue cones in the most proximal layer of the avian OPL (Günther et al., 2021; Mariani, 1987). To facilitate the identification based on PSD95, we used the peripheral retina because photoreceptors become less numerous and larger with increasing eccentricity.

Labeling for HCN1 in an EGFP-transfected retina revealed that HCN1+ ON bipolar cells contact rod and green and/or red cone photoreceptors (Figure 11a). The dendritic contact to the green/red cone was clearly invaginating the cone terminal whereas the invagination into the rod terminal was less obvious.

Labeling for PSD95 and PKC α showed that PKC α + bipolar cells contact double cones and potentially other photoreceptor types (Figure 11b, arrowheads) but avoid the most proximally stratifying

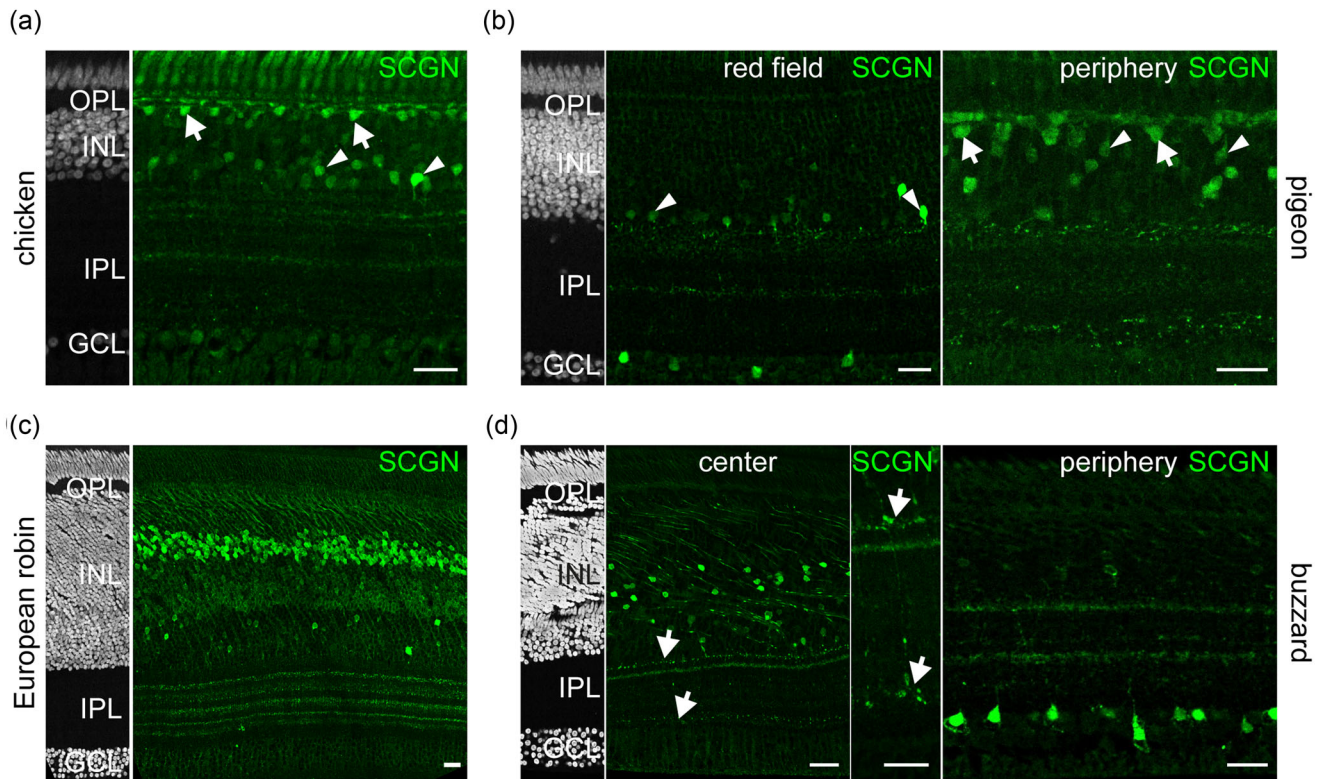


FIGURE 8 Secretagogin (SCGN) is a marker for bipolar cells in European robin and central buzzard retina. Labeling for SCGN in chicken (a), pigeon (b), European robin (c) and buzzard retina (d). In chicken retina, many retinal cell classes are labeled, particularly horizontal cells (arrows) and amacrine cells (arrowheads). In pigeon (b), the SCGN pattern of the peripheral retina resembles the staining in chicken (a) with a few bipolar cells labeled (arrowheads). In the pigeon red field, however, only amacrine and ganglion cells are strongly labeled. In the European robin retina (c), SCGN prominently labels bipolar cells and a few amacrine cells. SCGN expression differs between central and peripheral buzzard retina (d). In the central part, it resembles the European robin with many bipolar cells labeled. In the peripheral part, it resembles the staining in the pigeon red field with some amacrine and ganglion cells prominently stained. The bipolar cells in the central retina are clearly bistratified with terminals in the most distal and deep proximal layer of the inner plexiform layer (shown in higher magnification in the middle panel, arrows). DAPI labeled sections on the left side of the immunostainings serve to reveal the cell nuclei and retina layers (a–d). GCL, ganglion cell layer; INL, inner nuclear layer; IPL, inner plexiform layer; OPL, outer plexiform layer. Scale: 20 μ m

photoreceptor terminals (presumably UV/blue cones, Figure 11b, arrow). However, as PKC α + bipolar cells comprise several types with distinct stratification pattern in the IPL (see Figure 11b), we could not assign photoreceptor contacts to individual bipolar cell types.

CD15+ bipolar cells possess very wide-field dendritic trees in the peripheral European robin retina and contact rods and double cones (accessory member shown in Figure 12a, principal member shown in Figure 12b). Similar to PKC α + bipolar cells, they seem to avoid the most proximally stratifying photoreceptors (UV/blue cones, Figure 12b). Whether or not these bipolar cells contact green/red cones, we could not resolve.

4 | DISCUSSION

Bipolar cells collect photoreceptor signals and mediate them to retinal ganglion cells, transforming photoreceptor signals into many separate information channels encoding stimulus properties, such as contrast, color (reviewed in Euler et al., 2014), and—in case of night-migratory songbirds—potentially also magnetic field inclination (Hore &

Mouritsen, 2016; Wiltshcko et al., 1993; Zapka et al., 2009). The exact number of bipolar cell channels (= types) in the avian retina is not clear so far, with numbers ranging from 15 to 22 for the chicken, based on serial EM reconstructions (Günther et al., 2021) and transcriptomics (Yamagata et al., 2021), respectively. To get a better understanding of bipolar cells in the avian retina, we screened for markers which label individual bipolar cell types. Of the 12 markers we tested (in addition to *Islet1* and *GNB3*), we identified eight to reliably label bipolar cells in four different avian species. While no marker (except for *HCN1*) was specific to a single bipolar cell type, the markers we used still help segregate bipolar cells into types in avian retinæ, and the markers showed that the same markers do not always mark the same cell types in all birds.

4.1 | ON versus OFF bipolar cells in the avian retina

GNB3 and *Islet1* were found to colocalize in all avian species and served as reliable marker for ON bipolar cells (Ritchey et al., 2010; Yamagata et al., 2021). However, as *Islet1* was also detected in

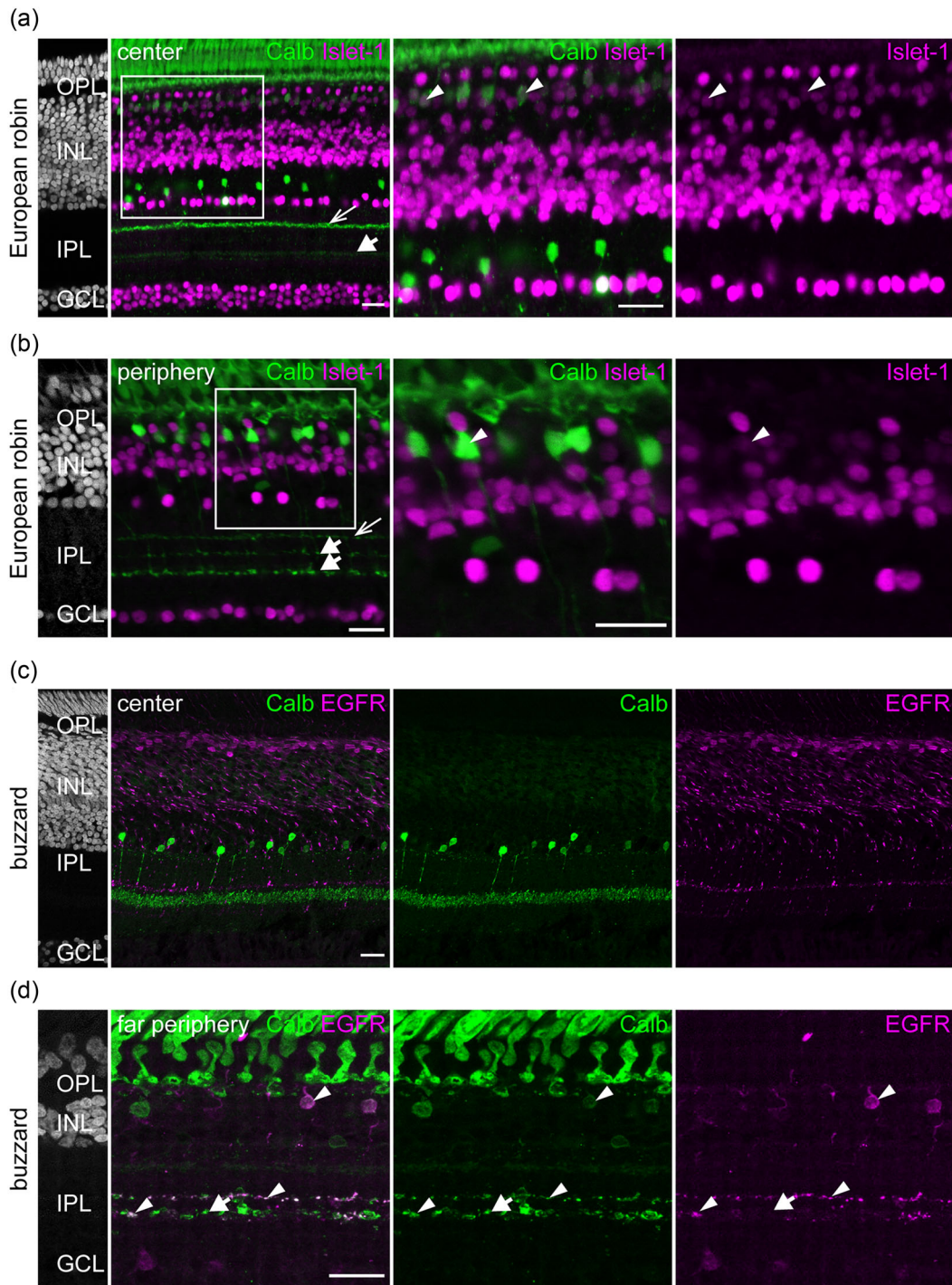


FIGURE 9 Calbindin differentially labels bipolar cells in the peripheral and central European robin and buzzard retina. Labeling for calbindin (Calb) and Islet1 in the central (a) and peripheral (b) European robin retina (a, b). In the central retina, Calb+/Islet1+ ON bipolar cells are only labeled in the soma (arrowheads). Additionally, a faint band is visible in the inner plexiform layer (IPL, short arrow). In contrast, in the periphery, the entire morphology, including the axon terminal stratification of Calb+/Islet1+ ON bipolar cells can be discerned (b, short arrows). Please note that the very prominent Calb+ band in the IPL of the central European robin retina originates from amacrine cells (a, thin arrow). This band is weaker in the peripheral retina (b, thin arrow). Calb and EGFR labeling in the central (c) and peripheral (d) buzzard retina reveal prominent Calb+ amacrine cells in the central retina and Calb+/EGFR+ bipolar cells in the far peripheral retina. These putative ON bipolar cells (see Figure 7d) show two distinct stratification bands in the middle of the inner plexiform layer (IPL) and resemble two populations with axon terminals which are either Calb+/EGFR+ (arrowheads) or Calb+/EGFR- (arrow). DAPI labeled sections on the left side of the immunostainings serve to reveal the cell nuclei and retina layers (a-d). GCL, ganglion cell layer; INL, inner plexiform layer; OPL, outer plexiform layer. Scale: 20 μ m

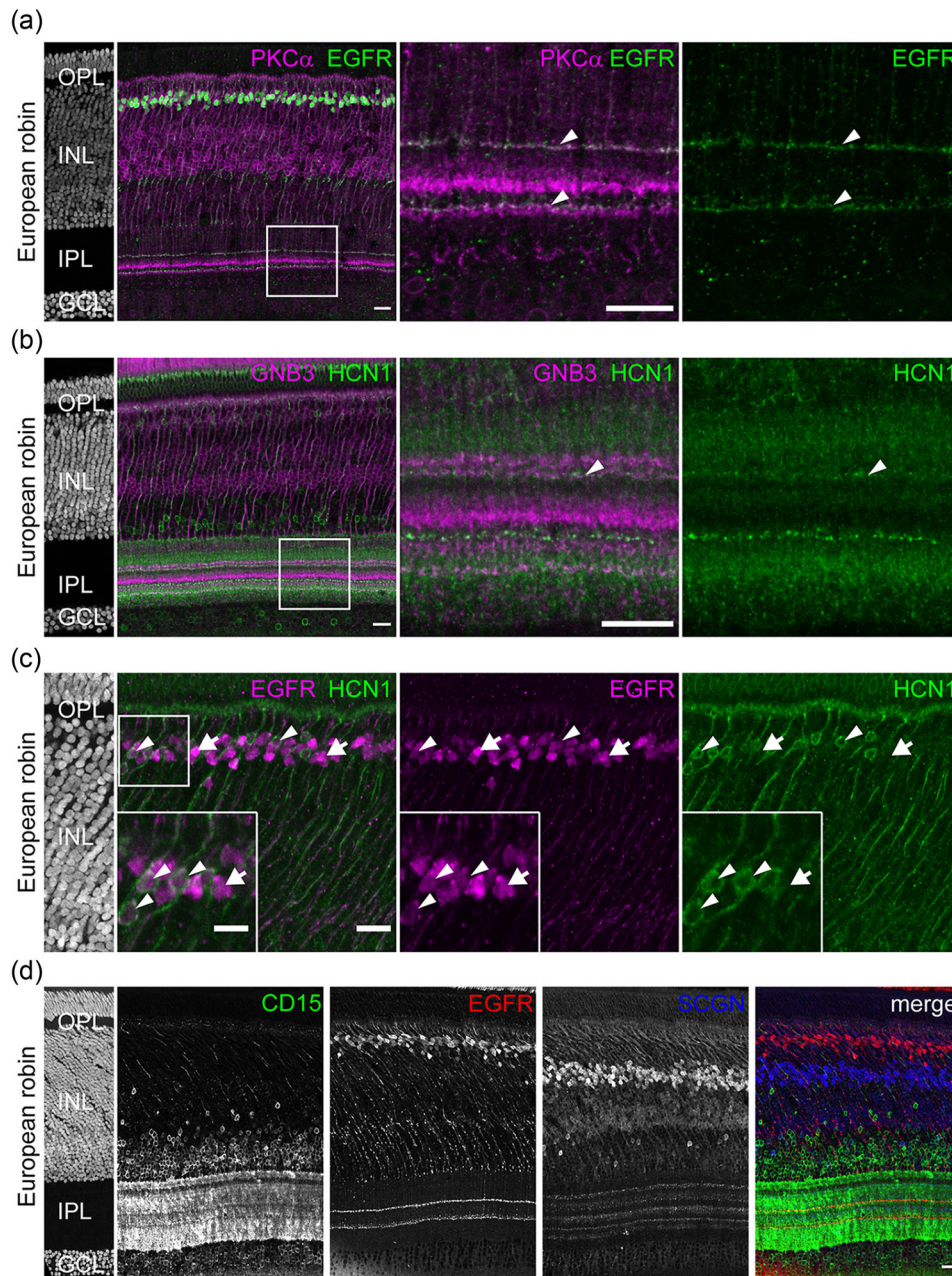


FIGURE 10 Markers for bipolar cells in the European robin retina. (a) Double-labeling for EGFR and PKC α revealed that EGFR+ bipolar cells are a subset of PKC α + bipolar cells. (b) Antibodies against HCN1 labeled several bands in the inner plexiform layer (IPL). The distal band is GNB3+ and belongs to HCN1+ bipolar cells. The bright proximal band (arrowheads) is GNB3- and likely originates from HCN1+ amacrine cells. (c) Double-labeling for EGFR and HCN1 revealed that HCN1+ bipolar cells represent a subset of EGFR+ bipolar cells. Arrows point to EGFR+/HCN1- bipolar cells; arrowheads indicate EGFR+/HCN1+ bipolar cells. Area marked by the white box is shown as insets in higher magnification. (d) Antibodies against CD15, EGFR, and SCGN label separate types of bipolar cells in the European robin retina. DAPI labeled sections on the left side of the immunostainings serve to reveal the cell nuclei and retina layers (a–d). GCL, ganglion cell layer; INL, inner nuclear layer; OPL, outer plexiform layer. Scale: 20 μ m, 10 μ m (inset)

ON-OFF bipolar cells in the chicken retina (Yamagata et al., 2021), we presume that these cells will be counted as ON bipolar cells in our study.

As already shown for the chicken retina (Günther et al., 2021), ON (GNB3+) layers were mainly confined to the proximal IPL, whereas

GNB3- layers were found in the distal half of the IPL and interspersed between ON (GNB3+) layers in the proximal half of the IPL in all four species (Figure 13). This suggests that the IPL organization is more diverse in avian species than in mammalian species where OFF layers are mostly restricted to the distal and ON layers to the proximal IPL

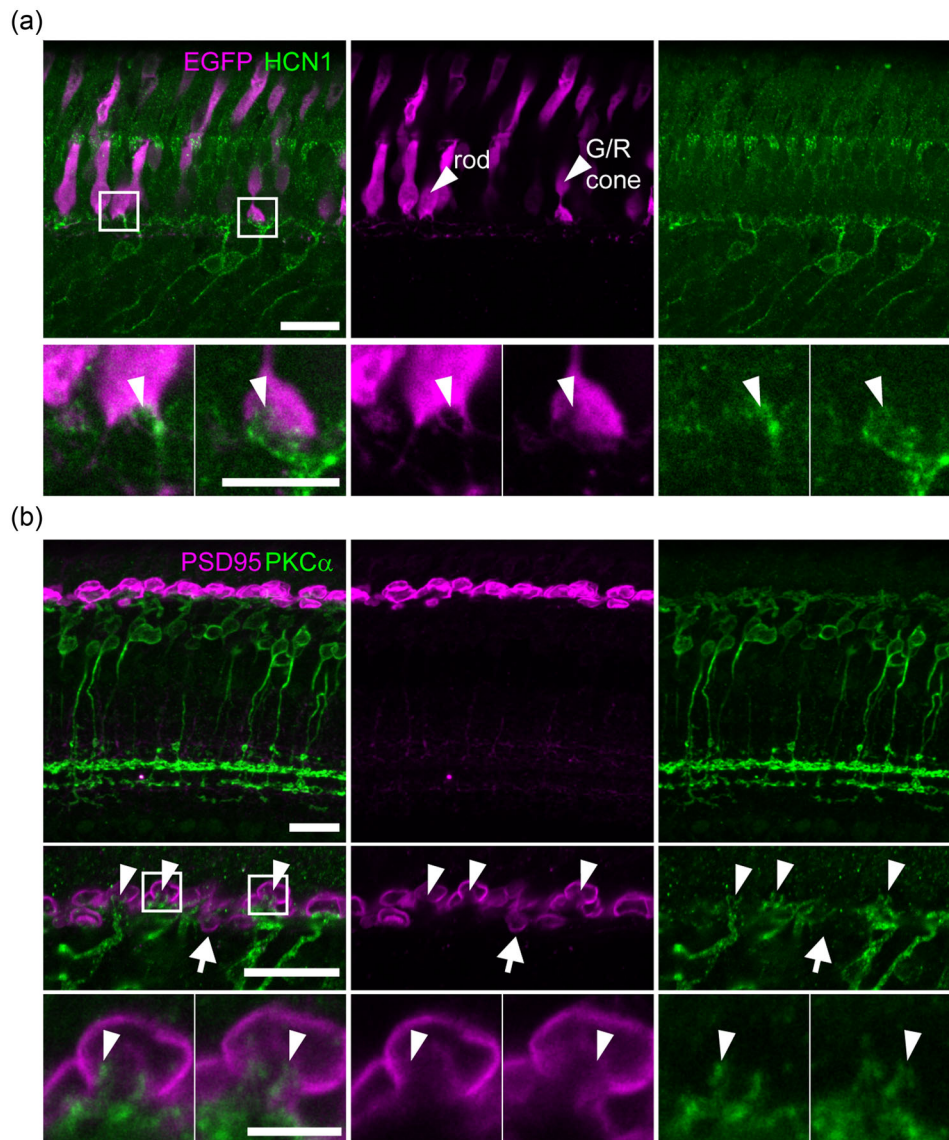


FIGURE 11 Photoreceptor contacts of HCN1+ and PKC α + bipolar cells in the European robin retina. (a) AAV-transfection leads to EGFP expression in different photoreceptors of the European robin retina. Double-labeling for EGFP and HCN1 revealed that HCN1+ bipolar cells contact rod photoreceptors and green and/or red photoreceptors (based on photoreceptor terminal shape and stratification depth in the outer plexiform layer, Günther et al., 2021). Arrowheads mark contact points (invaginations). (b) Staining for PKC α and PSD95 in the very peripheral European robin retina allowed discerning photoreceptor contacts of PKC α + bipolar cells: they contact double cone photoreceptors (arrowheads) and avoid putative UV/blue cones (arrow). However, as PKC α + bipolar cells likely comprise several types with different stratification pattern in the inner plexiform layer, assigning contacts to individual types is not possible at light microscopical resolution. White squares mark areas shown in high magnification as single confocal scans. Scale: 20 μ m (a, b), 10 μ m (b), 5 μ m (a, b)

(with few exceptions: Dumitrescu et al., 2009; Hoshi et al., 2009). This makes the bird retina more similar to other vertebrate classes because OFF bipolar cells stratifying in the OFF and ON layer exist also in turtle (Ammermüller & Kolb, 1995) and fish retina (Connaughton & Nelson, 2000).

As all markers, except for CD15, labeled Islet1+ bipolar cells in the four avian species, we presumed that ON bipolar cells may outnumber OFF bipolar cells in the bird retina. This seemed particularly true for the European robin retina in which ON bipolar cells are arranged in three distinct layers in the INL (see Figures 2c and 3a) and indeed,

when we quantified the number of ON bipolar cells versus OFF bipolar cells in the central European robin and chicken retina, we found slightly more ON (~55%) than OFF bipolar cells (~45%) in both species. These numbers are very similar to numbers from the mouse retina: Helmstaedter et al. (2013) reconstructed 144 OFF cone (47%) and 163 ON cone bipolar cells (53%) from a serial electron microscopy stack of the mouse retina. However, there are two caveats for our data: (1) ON bipolar cells are slightly overestimated because Islet1+ cells will not only comprise ON but also the single type of ON-OFF bipolar cells present at least in chicken (Yamagata et al., 2021); (2) OFF

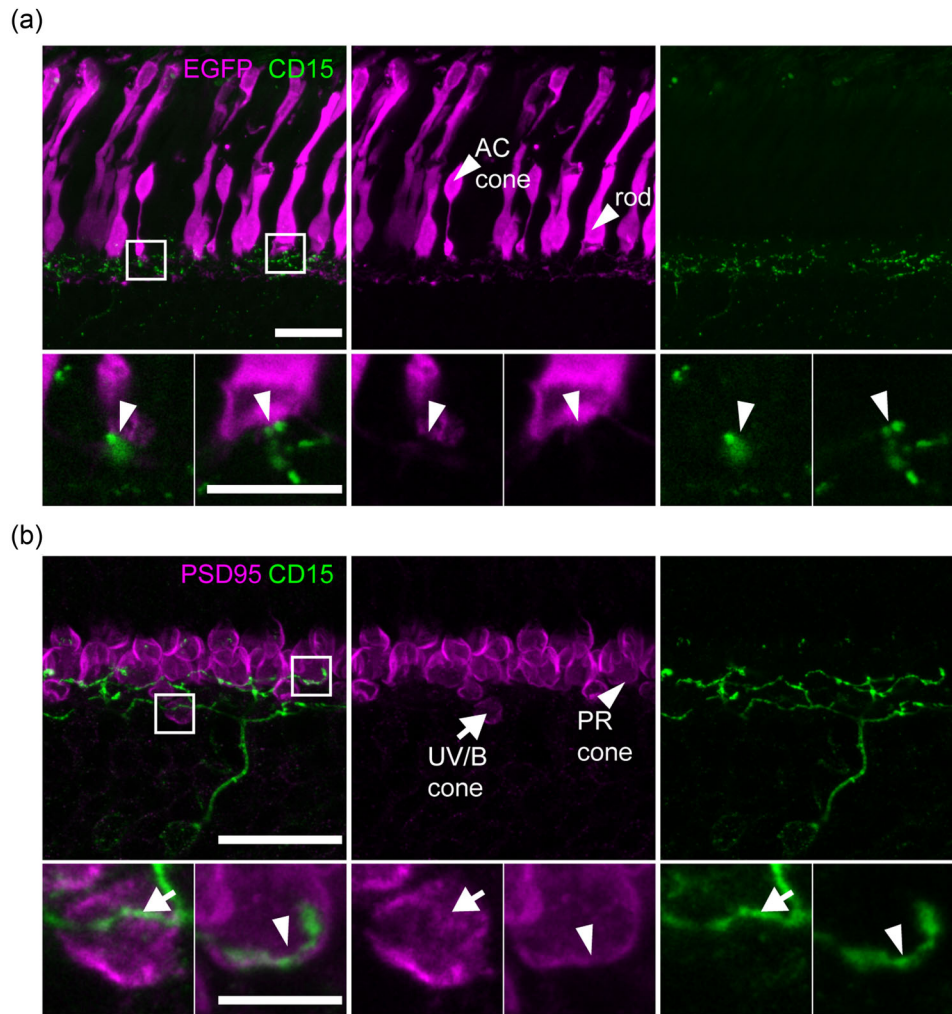


FIGURE 12 Photoreceptor contacts of CD15+ bipolar cells in the European robin retina. (a) Double-labeling for EGFP and CD15 in an AAV-transfected European robin retina revealed contact points between CD15+ bipolar cells and rods and the accessory member of the double cone (AC). (b) Staining for CD15 and PSD95 in the peripheral European robin retina showed that CD15+ bipolar cells are wide-field cells. In addition to rods and AC (a), they contact the principal member of the double cone (PR, arrowheads) and avoid UV and/or blue cones (UV/B cone, arrow, assignment based on photoreceptor terminal shape and stratification depth in the outer plexiform layer, Günther et al., 2021). White squares mark magnified areas, which are shown as single confocal scans. Scale: 20 μm , 5 μm

bipolar cells are slightly overestimated because Islet1⁻/Pax⁻ nuclei may also comprise the nuclei of Müller cells. However, if there is indeed a bias towards more ON bipolar cells (factor 1.2), the bias may be counterbalanced by the higher number of ribbon synapses we found in OFF bipolar cell terminals compared to ON bipolar cell terminals (factor 1.2–1.3). Also, differences in synapse size and strength may compensate it.

4.2 | Specificity of bipolar cell markers and comparison across species

As most markers not only labeled bipolar cells but also other cell types in the avian retina, we made no attempt to relate the different markers to our recently published bipolar cell classification of the chicken retina

(Günther et al., 2021). Notably, the staining pattern for most markers (CD15, PKC α , PKC β , SCGN; Table 2) differed between avian species, with the least differences for EGFR and HCN1.

CD15 was the only marker for Islet1⁻ OFF bipolar cells (chicken, European robin, buzzard) that we found. However, CD15 antibodies also labeled ON bipolar cells in three species (chicken, pigeon, European robin). In the pigeon retina, a wide-field ON bipolar cell was labeled.

Antibodies against PKC α and PKC β labeled many different bipolar cell types in European robin and buzzard retina whereas only a few types are labeled by PKC α in the chicken retina (Caminos et al., 1999; Günther et al., 2021; Koulen et al., 1997). In the European robin, PKC α and PKC β labeling largely overlapped with GNB3 labeling suggesting that mostly ON bipolar cells are labeled. In the peripheral buzzard retina, GNB3 and PKC α largely overlap (as in the European robin),

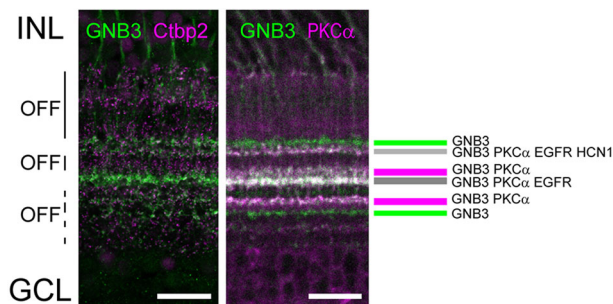


FIGURE 13 Organization of the inner plexiform layer of the European robin retina. Schematic representation revealing the complex organization of the inner plexiform layer of the bird retina, based on stainings for GNB3 (Figure 2), PKC α (Figure 4), EGFR (Figures 7 and 10), and HCN1 (Figures 6 and 10) in the European robin. Assignments of ON and OFF layers are based on GNB3 and Ctbp2 labeling. GCL, ganglion cell layer; INL, inner nuclear layer. Scale: 20 μ m

and we see additional bands with PKC β due to the labeled amacrine cells.

Antibodies against EGFR were originally expected to label one type of horizontal cell, a few bipolar and ganglion cell types, and possibly rods based on transcriptomic data (Yamagata et al., 2021) but were found to be the only marker which exclusively labeled bipolar cells in all avian species. Double-labeling with HCN1 revealed for European robin that EGFR+ bipolar cells fall into two different types, one that is monostratified and HCN1+ and one that is HCN1-. The HCN+/EGFR+ ON bipolar cells stratifying more distally are also positive for PKC α , whereas HCN1-/EGFR+ ON bipolar cells are not (please compare Figures 4a and 10b). The various combinations of HCN1, EGFR, PKC α , and GNB3 antibodies allowed us to separate the six GNB3+ bands in the IPL of the European robin (please see Figure 4a together with Figure 13). This analysis suggests that the IPL organization is very complex in avian species and may not be captured well by the classical division into eight equidistant strata (Günther et al., 2021; Naito & Chen, 2004).

4.3 | Regional differences in expression of bipolar cell markers

Bird retinæ showed marked regional differences in immunoreactivity. For example, calbindin only labeled bipolar cells in the peripheral retina in the European robin and buzzard, consistent with an earlier report from chicken (Rogers, 1989). Similarly, SCGN staining showed marked differences between peripheral and central retina in buzzard and pigeon retina, with SCGN+ bipolar cells occurring only in the central or peripheral retina, respectively.

It remains unclear whether this reflects the differential expression of calcium-binding proteins in different regions of the bird retina or the inhomogeneous distribution of certain bipolar cell types across the retina. In any case, these topographic differences may reflect species-specific adaptations to different visual environments (Baden et al., 2020).

4.4 | Photoreceptor connections of selected bipolar cell types in the European robin retina

Photoreceptors may be the initiation point for magnetoreception in night-migratory songbirds. As the best supported sensory molecule, cryptochrome 4 (Xu et al., 2021), is expressed in the outer and inner segments of double cones and long-wavelength single cones in the European robin retina (Chetverikova et al., 2022; Günther et al., 2018), we were also interested in finding bipolar cells that contact these photoreceptors because they may carry magnetic signals in addition to visual signals. However, only three bipolar cell markers were suitable for assessing the photoreceptor connections. HCN1+ ON bipolar cells invaginate the terminals of green and/or red cones. Both cone types stratify in the same layer of the OPL so that we could not differentiate between the two. Additionally, HCN1+ bipolar cells also contacted rod photoreceptors. For the other photoreceptor types, we cannot draw any firm conclusions because we only had a selected number of photoreceptors that expressed EGFP. For PKC α + bipolar cells, however, we assume that they avoid UV/blue cones because we did not see any PKC α -labeled processes that contacted PSD95-labeled photoreceptor terminals in the most proximal layer of the OPL. Instead, we provide evidence that PKC α -labeled bipolar cells invaginate double cones. CD15+ bipolar cells have large dendritic trees and are likely wide-field bipolar cells in the European robin retina. They also contact double cones while avoiding UV/blue cones. Whether or not they also sample from green and/or red cones, we could not discern. Other types of studies (like volume EM reconstructions) are needed to determine the bipolar cell types postsynaptic to double cones in the European robin retina.

AUTHOR CONTRIBUTIONS

KD and SH designed the project; VB, SH, PKS, AG, JS, MH, LLP, PN, and EM performed experiments; VB, KD, SH, and AG analyzed data; KD, SH, HM, and CS supervised the project; KD, SH, and VB prepared figures; KD wrote the manuscript; all authors commented on the manuscript and KD finalized it.

ACKNOWLEDGMENTS

We thank Irina Fomins and Ursula Kobalz for their excellent technical assistance and Dr. Beate Grünberg and Dr. Tina Schlüter for their organizational support. The authors also acknowledge the Service Unit (Core Facility) Fluorescence Microscopy of the University of Oldenburg, Oldenburg, and the Viral Core Facility of Charité—Universitätsmedizin Berlin, Germany. This work was funded by the Deutsche Forschungsgemeinschaft (SFB1372: *Navigation and Magnetoreception in Vertebrates*, project number: 395940726 and RTG 1885/2 *Molecular Basis of Sensory Biology* to KD and HM) and the Czech Science Foundation, project number: 22-35153S, to PN. HM also acknowledges funding from the European Research Council (under the European Union's Horizon 2020 research and innovation programme, grant agreement no. 810002 (Synergy Grant: *QuantumBirds*). AG is grateful for central funding from the Presidential Board of the

University of Oldenburg. In addition, funding was obtained from Stiftung Caesar and the Max Planck Society.

Open Access funding enabled and organized by Projekt DEAL.

CONFLICT OF INTEREST

The authors declare that there are no potential sources of conflict of interest.

DATA AVAILABILITY STATEMENT

The data that support the findings of this study are available from the corresponding author upon reasonable request.

ORCID

Pranav Kumar Seth  <https://orcid.org/0000-0002-5710-4607>

Anja Günther  <https://orcid.org/0000-0003-1724-3298>

Ezequiel Mendoza  <https://orcid.org/0000-0003-4963-519X>

Jessica Schmidt  <https://orcid.org/0000-0002-8393-4532>

Pavel Němec  <https://orcid.org/0000-0003-0277-0239>

Constance Scharff  <https://orcid.org/0000-0002-5792-076X>

Henrik Mouritsen  <https://orcid.org/0000-0001-7082-4839>

Karin Dedek  <https://orcid.org/0000-0003-1490-0141>

REFERENCES

- Ammermüller, J., & Kolb, H. (1995). The organization of the turtle inner retina. I. ON- and OFF-center pathways. *The Journal of Comparative Neurology*, 358(1), 1–34. <https://doi.org/10.1002/cne.903580102>
- Ammermüller, J., Müller, J. F., & Kolb, H. (1995). The organization of the turtle inner retina. II. Analysis of color-coded and directionally selective cells. *The Journal of Comparative Neurology*, 358(1), 35–62. <https://doi.org/10.1002/cne.903580103>
- Baden, T., Euler, T., & Berens, P. (2020). Understanding the retinal basis of vision across species. *Nature Reviews Neuroscience*, 21(1), 5–20. <https://doi.org/10.1038/s41583-019-0242-1>
- Behrens, C., Schubert, T., Haverkamp, S., Euler, T., & Berens, P. (2016). Connectivity map of bipolar cells and photoreceptors in the mouse retina. *eLife*, 5, e20041. <https://doi.org/10.7554/eLife.20041>
- Breuninger, T., Puller, C., Haverkamp, S., & Euler, T. (2011). Chromatic bipolar cell pathways in the mouse retina. *The Journal of Neuroscience*, 31(17), 6504–6517. <https://doi.org/10.1523/JNEUROSCI.0616-11.2011>
- Caminos, E., Velasco, A., Jarrín, M., Aijón, J., & Lara, J. M. (1999). Protein kinase C-like immunoreactive cells in embryo and adult chicken retinas. *Brain Research. Developmental Brain Research*, 118(1–2), 227–230. [https://doi.org/10.1016/s0165-3806\(99\)00156-x](https://doi.org/10.1016/s0165-3806(99)00156-x)
- Chan, T. L., Martin, P. R., Clunas, N., & Grünert, U. (2001). Bipolar cell diversity in the primate retina: Morphologic and immunocytochemical analysis of a new world monkey, the marmoset *Callithrix jacchus*. *The Journal of Comparative Neurology*, 437(2), 219–239. <https://doi.org/10.1002/cne.1280>
- Chetverikova, R., Dautaj, G., Schwigon, L., Dedek, K., & Mouritsen, H. (2022). Double cones in the avian retina form an oriented mosaic which might facilitate magnetoreception and/or polarized light sensing. *Journal of The Royal Society Interface*, 19(189), 20210877. <https://doi.org/10.1098/rsif.2021.0877>
- Connaughton, V. P., & Nelson, R. (2000). Axonal stratification patterns and glutamate-gated conductance mechanisms in zebrafish retinal bipolar cells. *The Journal of Physiology*, 524 Pt 1, 135–146. <https://doi.org/10.1111/j.1469-7793.2000.t01-1-00135.x>
- Della Santina, L., Kuo, S. P., Yoshimatsu, T., Okawa, H., Suzuki, S. C., Hoon, M., Tsuboyama, K., Rieke, F., & Wong, R. O. L. (2016). Glutamatergic monopolar interneurons provide a novel pathway of excitation in the mouse retina. *Current Biology*, 26(15), 2070–2077. <https://doi.org/10.1016/j.cub.2016.06.016>
- DeVries, S. H. (2000). Bipolar cells use kainate and AMPA receptors to filter visual information into separate channels. *Neuron*, 28(3), 847–856. [https://doi.org/10.1016/S0896-6273\(00\)00158-6](https://doi.org/10.1016/S0896-6273(00)00158-6)
- Dudczig, S., Currie, P. D., & Jusuf, P. R. (2017). Developmental and adult characterization of secretagogin expressing amacrine cells in zebrafish retina. *PLOS ONE*, 12(9), e0185107. <https://doi.org/10.1371/journal.pone.0185107>
- Dumitrescu, O. N., Pucci, F. G., Wong, K. Y., & Berson, D. M. (2009). Ectopic retinal ON bipolar cell synapses in the OFF inner plexiform layer: Contacts with dopaminergic amacrine cells and melanopsin ganglion cells. *The Journal of Comparative Neurology*, 517(2), 226–244. <https://doi.org/10.1002/cne.22158>
- Euler, T., Haverkamp, S., Schubert, T., & Baden, T. (2014). Retinal bipolar cells: Elementary building blocks of vision. *Nature Reviews Neuroscience*, 15(8), 507–519. <https://doi.org/10.1038/nrn3783>
- Fischer, A. J., Foster, S., Scott, M. A., & Sherwood, P. (2008). Transient expression of LIM-domain transcription factors is coincident with delayed maturation of photoreceptors in the chicken retina. *The Journal of Comparative Neurology*, 506(4), 584–603. <https://doi.org/10.1002/cne.21578>
- Fischer, A. J., Stanke, J. J., Aloisio, G., Hoy, H., & Stell, W. K. (2007). Heterogeneity of horizontal cells in the chicken retina. *The Journal of Comparative Neurology*, 500(6), 1154–1171. <https://doi.org/10.1002/cne.21236>
- Fournel, R., Hartveit, E., & Veruki, M. L. (2021). Differential contribution of gap junctions to the membrane properties of ON- and OFF-bipolar cells of the rat retina. *Cellular and Molecular Neurobiology*, 41(2), 229–245. <https://doi.org/10.1007/s10571-020-00845-y>
- Franke, K., Berens, P., Schubert, T., Bethge, M., Euler, T., & Baden, T. (2017). Inhibition decorrelates visual feature representations in the inner retina. *Nature*, 542(7642), 439–444. <https://doi.org/10.1038/nature21394>
- Ghosh, K. K., Bujan, S., Haverkamp, S., Feigenspan, A., & Wässle, H. (2004). Types of bipolar cells in the mouse retina. *The Journal of Comparative Neurology*, 469(1), 70–82. <https://doi.org/10.1002/cne.10985>
- Günther, A., Dedek, K., Haverkamp, S., Irsen, S., Briggman, K. L., & Mouritsen, H. (2021). Double cones and the diverse connectivity of photoreceptors and bipolar cells in an avian retina. *The Journal of Neuroscience: The Official Journal of the Society for Neuroscience*, 41(23), 5015–5028. <https://doi.org/10.1523/JNEUROSCI.2495-20.2021>
- Günther, A., Einwich, A., Sjulstok, E., Feederle, R., Bolte, P., Koch, K.-W., Solov'yov, I. A., & Mouritsen, H. (2018). Double-cone localization and seasonal expression pattern suggest a role in magnetoreception for European Robin cryptochrome 4. *Current Biology: CB*, 28(2), 211–223.e4. <https://doi.org/10.1016/j.cub.2017.12.003>
- Haug, M. F., Berger, M., Gesemann, M., & Neuhaus, S. C. F. (2019). Differential expression of PKC α and β in the zebrafish retina. *Histochemistry and Cell Biology*, 151(6), 521–530. <https://doi.org/10.1007/s00418-018-1764-8>
- Haverkamp, S., Albert, L., Balaji, V., Němec, P., & Dedek, K. (2021). Expression of cell markers and transcription factors in the avian retina compared with that in the marmoset retina. *The Journal of Comparative Neurology*, 529(12), 3171–3193. <https://doi.org/10.1002/cne.25154>
- Haverkamp, S., Ghosh, K. K., Hirano, A. A., & Wässle, H. (2003a). Immunocytochemical description of five bipolar cell types of the mouse retina. *The Journal of Comparative Neurology*, 455(4), 463–476. <https://doi.org/10.1002/cne.10491>
- Haverkamp, S., Haeseleer, F., & Hendrickson, A. (2003b). A comparison of immunocytochemical markers to identify bipolar cell types in human and monkey retina. *Visual Neuroscience*, 20(6), 589–600. <https://doi.org/10.1017/S0952523803206015>
- Haverkamp, S., & Wässle, H. (2000). Immunocytochemical analysis of the mouse retina. *The Journal of Comparative Neurology*, 424(1), 1–23.

- Haverkamp, S., Wässle, H., Duebel, J., Kuner, T., Augustine, G. J., Feng, G., & Euler, T. (2005). The primordial, blue-cone color system of the mouse retina. *The Journal of Neuroscience*, 25(22), 5438–5445. <https://doi.org/10.1523/JNEUROSCI.1117-05.2005>
- Haverkamp, S., Specht, D., Majumdar, S., Zaidi, N. F., Brandstätter, J. H., Wasco, W., Wässle, H., & Tom Dieck, S. (2008). Type 4 OFF cone bipolar cells of the mouse retina express calnexin and contact cones as well as rods. *J. Comp. Neurol.*, 507, 1087–101. <https://doi.org/10.1002/cne.21612>. PMID:18095322
- Hellmer, C. B., Zhou, Y., Fyk-Kolodziej, B., Hu, Z., & Ichinose, T. (2016). Morphological and physiological analysis of type-5 and other bipolar cells in the mouse retina. *Neuroscience*, 315, 246–258. <https://doi.org/10.1016/j.neuroscience.2015.12.016>
- Helmstaedter, M., Briggman, K. L., Turaga, S. C., Jain, V., Seung, H. S., & Denk, W. (2013). Connectomic reconstruction of the inner plexiform layer in the mouse retina. *Nature*, 500(7461), 168–174. <https://doi.org/10.1038/nature12346>
- Heyers, D., Manns, M., Luksch, H., Güntürkün, O., & Mouritsen, H. (2007). A visual pathway links brain structures active during magnetic compass orientation in migratory birds. *PLoS One*, 2(9), e937. <https://doi.org/10.1371/journal.pone.0000937>
- Hore, P. J., & Mouritsen, H. (2016). The radical-pair mechanism of magnetoreception. *Annual Review of Biophysics*, 45, 299–344. <https://doi.org/10.1146/annurev-biophys-032116-094545>
- Hoshi, H., Liu, W.-L., Massey, S. C., & Mills, S. L. (2009). ON inputs to the OFF layer: Bipolar cells that break the stratification rules of the retina. *The Journal of Neuroscience: The Official Journal of the Society for Neuroscience*, 29(28), 8875–8883. <https://doi.org/10.1523/JNEUROSCI.0912-09.2009>
- Hübner, D., Rankovic, M., Richter, K., Lazarevic, V., Altmann, W. D., Fischer, K.-D., Gundelfinger, E. D., & Fejtova, A. (2012). Differential spatial expression and subcellular localization of CtBP family members in rodent brain. *PLOS ONE*, 7(6), e39710. <https://doi.org/10.1371/journal.pone.0039710>
- Ichinose, T., & Hellmer, C. B. (2016). Differential signalling and glutamate receptor compositions in the OFF bipolar cell types in the mouse retina. *The Journal of Physiology*, 594(4), 883–894. <https://doi.org/10.1113/JP271458>
- Ivanova, E., & Müller, F. (2006). Retinal bipolar cell types differ in their inventory of ion channels. *Visual Neuroscience*, 23(2), 143–154. <https://doi.org/10.1017/S0952523806232048>
- Kim, I.-B., Lee, E.-J., Kang, T.-H., Chung, J.-W., & Chun, M.-H. (2003). Morphological analysis of the hyperpolarization-activated cyclic nucleotide-gated cation channel 1 (HCN1) immunoreactive bipolar cells in the rabbit retina. *The Journal of Comparative Neurology*, 467(3), 389–402. <https://doi.org/10.1002/cne.10957>
- Koulen, P., Brandstätter, J. H., Kröger, S., Enz, R., Bormann, J., & Wässle, H. (1997). Immunocytochemical localization of the GABAC receptor ρ subunits in the cat, goldfish, and chicken retina. *Journal of Comparative Neurology*, 380(4), 520–532. [https://doi.org/10.1002/\(SICI\)1096-9861\(19970421\)380:4:520::AID-CNE8/3.0.CO;2-3](https://doi.org/10.1002/(SICI)1096-9861(19970421)380:4:520::AID-CNE8/3.0.CO;2-3)
- Koulen, P., Fletcher, E. L., Craven, S. E., Bredt, D. S., & Wässle, H. (1998). Immunocytochemical localization of the postsynaptic density protein PSD-95 in the mammalian retina. *The Journal of Neuroscience*, 18(23), 10136–10149. <https://doi.org/10.1523/JNEUROSCI.18-23-10136.1998>
- Kverková, K., Marhounová, L., Polonyiová, A., Kocourek, M., Zhang, Y., Olkowicz, S., Straková, B., Pavelková, Z., Vodička, R., Frynta, D., & Němec, P. (2022). The evolution of brain neuron numbers in amniotes. *Proceedings of the National Academy of Sciences of the United States of America*, 119(11), e2121624119. <https://doi.org/10.1073/pnas.2121624119>
- Li, Y. N., Tsujimura, T., Kawamura, S., & Dowling, J. E. (2012). Bipolar cell-photoreceptor connectivity in the zebrafish (*Danio rerio*) retina. *The Journal of comparative neurology*, 520(16), 3786–3802. <https://doi.org/10.1002/cne.23168>
- Liedvogel, M., Feenders, G., Wada, K., Troje, N. F., Jarvis, E. D., & Mouritsen, H. (2007). Lateralized activation of Cluster N in the brains of migratory songbirds. *The European Journal of Neuroscience*, 25(4), 1166–1173. <https://doi.org/10.1111/j.1460-9568.2007.05350.x>
- Mariani, A. P. (1987). Neuronal and synaptic organization of the outer plexiform layer of the pigeon retina. *The American Journal of Anatomy*, 179(1), 25–39. <https://doi.org/10.1002/aja.1001790105>
- Mataruga, A., Kremmer, E., & Müller, F. (2007). Type 3a and type 3b OFF cone bipolar cells provide for the alternative rod pathway in the mouse retina. *The Journal of Comparative Neurology*, 502(6), 1123–1137. <https://doi.org/10.1002/cne.21367>
- Mouritsen, H. (2018). Long-distance navigation and magnetoreception in migratory animals. *Nature*, 558(7708), 50–59. <https://doi.org/10.1038/s41586-018-0176-1>
- Mouritsen, H., Feenders, G., Liedvogel, M., Wada, K., & Jarvis, E. D. (2005). Night-vision brain area in migratory songbirds. *Proceedings of the National Academy of Sciences of the United States of America*, 102(23), 8339–8344. <https://doi.org/10.1073/pnas.0409575102>
- Naito, J., & Chen, Y. (2004). Morphological features of chick retinal ganglion cells. *Anatomical Science International*, 79(4), 213–225. <https://doi.org/10.1111/j.1447-073x.2004.00084.x>
- Pasteels, B., Rogers, J., Blachier, F., & Pochet, R. (1990). Calbindin and calretinin localization in retina from different species. *Visual Neuroscience*, 5(1), 1–16. <https://doi.org/10.1017/S0952523800000031>
- Pignatelli, V., & Strettoi, E. (2004). Bipolar cells of the mouse retina: A gene gun, morphological study. *The Journal of Comparative Neurology*, 476(3), 254–266. <https://doi.org/10.1002/cne.20207>
- Prum, R. O., Berv, J. S., Dornburg, A., Field, D. J., Townsend, J. P., Lemmon, E. M., & Lemmon, A. R. (2015). A comprehensive phylogeny of birds (Aves) using targeted next-generation DNA sequencing. *Nature*, 526(7574), Art. 7574. <https://doi.org/10.1038/nature15697>
- Puller, C., Ivanova, E., Euler, T., Haverkamp, S., & Schubert, T. (2013). OFF bipolar cells express distinct types of dendritic glutamate receptors in the mouse retina. *Neuroscience*, 243, 136–148. <https://doi.org/10.1016/j.neuroscience.2013.03.054>
- Puller, C., Ondreka, K., & Haverkamp, S. (2011). Bipolar cells of the ground squirrel retina. *Journal of Comparative Neurology*, 519(4), 759–774. <https://doi.org/10.1002/cne.22546>
- Puthussery, T., Gayet-Primo, J., & Taylor, W. R. (2010). Localization of the calcium-binding protein secretogin in cone bipolar cells of the mammalian retina. *The Journal of comparative neurology*, 518(4), <https://doi.org/10.1002/cne.22234>
- Puthussery, T., Gayet-Primo, J., Taylor, W. R., & Haverkamp, S. (2011). Immunohistochemical identification and synaptic inputs to the diffuse bipolar cell type DB1 in macaque retina. *Journal of Comparative Neurology*, 519(18), 3640–3656. <https://doi.org/10.1002/cne.22756>
- Quesada, A., Prada, F. A., & Genis-Galvez, J. M. (1988). Bipolar cells in the chicken retina. *Journal of Morphology*, 197(3), 337–351. <https://doi.org/10.1002/jmor.1051970308>
- Ritche, E. R., Bongini, R. E., Code, K. A., Zelinka, C., Petersen-Jones, S., & Fischer, A. J. (2010). The pattern of expression of guanine nucleotide-binding protein beta3 in the retina is conserved across vertebrate species. *Neuroscience*, 169(3), 1376–1391. <https://doi.org/10.1016/j.neuroscience.2010.05.081>
- Ritz, T., Adem, S., & Schulten, K. (2000). A model for photoreceptor-based magnetoreception in birds. *Biophysical Journal*, 78(2), 707–718. [https://doi.org/10.1016/S0006-3495\(00\)76629-X](https://doi.org/10.1016/S0006-3495(00)76629-X)
- Rogers, J. H. (1989). Two calcium-binding proteins mark many chick sensory neurons. *Neuroscience*, 31(3), 697–709. [https://doi.org/10.1016/0306-4522\(89\)90434-X](https://doi.org/10.1016/0306-4522(89)90434-X)
- Schindelin, J., Arganda-Carreras, I., Frise, E., Kaynig, V., Longair, M., Pietzsch, T., Preibisch, S., Rueden, C., Saalfeld, S., Schmid, B., Tinevez, J.-Y., White, D. J., Hartenstein, V., Eliceiri, K., Tomancak, P., & Cardona, A. (2012). Fiji: An open-source platform for biological-image analysis. *Nature Methods*, 9(7), 676–682. <https://doi.org/10.1038/nmeth.2019>

- Shekhar, K., Lapan, S. W., Whitney, I. E., Tran, N. M., Macosko, E. Z., Kowalczyk, M., Adiconis, X., Levin, J. Z., Nemes, J., Goldman, M., McCarroll, S. A., Cepko, C. L., Regev, A., & Sanes, J. R. (2016). Comprehensive classification of retinal bipolar neurons by single-cell transcriptomics. *Cell*, 166(5), 1308–1323.e30. <https://doi.org/10.1016/j.cell.2016.07.054>
- Stanke, J. J., Lehman, B., & Fischer, A. J. (2008). Muscarinic signaling influences the patterning and phenotype of cholinergic amacrine cells in the developing chick retina. *BMC Developmental Biology*, 8, 13. <https://doi.org/10.1186/1471-213X-8-13>
- Wässle, H., Puller, C., Müller, F., & Haverkamp, S. (2009). Cone contacts, mosaics, and territories of bipolar cells in the mouse retina. *The Journal of Neuroscience: The Official Journal of the Society for Neuroscience*, 29(1), 106–117. <https://doi.org/10.1523/JNEUROSCI.4442-08.2009>
- Weltzien, F., Dimarco, S., Protti, D. A., Daraio, T., Martin, P. R., & Grünert, U. (2014). Characterization of secretogin-immunoreactive amacrine cells in marmoset retina. *The Journal of Comparative Neurology*, 522(2), 435–455. <https://doi.org/10.1002/cne.23420>
- Wiltchko, W., Munro, U., Ford, H., & Wiltchko, R. (1993). Red light disrupts magnetic orientation of migratory birds. *Nature*, 364(6437), 525–527. <https://doi.org/10.1038/364525a0>
- Wiltchko, W., & Wiltchko, R. (1972). Magnetic compass of European robins. *Science (New York, N.Y.)*, 176(4030), 62–64. <https://doi.org/10.1126/science.176.4030.62>
- Wong, K. Y., & Dowling, J. E. (2005). Retinal bipolar cell input mechanisms in giant danio. III. ON-OFF bipolar cells and their color-opponent mechanisms. *Journal of Neurophysiology*, 94(1), 265–272. <https://doi.org/10.1152/jn.00271.2004>
- Xu, J., Jarocha, L. E., Zollitsch, T., Konowalczyk, M., Henbest, K. B., Richert, S., Golesworthy, M. J., Schmidt, J., Déjean, V., Sowood, D. J. C., Bassetto, M., Luo, J., Walton, J. R., Fleming, J., Wei, Y., Pitcher, T. L., Moise, G., Herrmann, M., Yin, H., ... Hore, P. J. (2021). Magnetic sensitivity of cryptochrome 4 from a migratory songbird. *Nature*, 594(7864), 535–540. <https://doi.org/10.1038/s41586-021-03618-9>
- Yamagata, M., Yan, W., & Sanes, J. R. (2021). A cell atlas of the chick retina based on single-cell transcriptomics. *ELife*, 10, e63907. <https://doi.org/10.7554/eLife.63907>
- Zapka, M., Heyers, D., Hein, C. M., Engels, S., Schneider, N.-L., Hans, J., Weiler, S., Dreyer, D., Kishkinev, D., Wild, J. M., & Mouritsen, H. (2009). Visual but not trigeminal mediation of magnetic compass information in a migratory bird. *Nature*, 461(7268), 1274–1277. <https://doi.org/10.1038/nature08528>

How to cite this article: Balaji, V., Haverkamp, S., Seth, P. K., Günther, A., Mendoza, E., Schmidt, J., Herrmann, M., Pfeiffer, L. L., Němec, P., Scharff, C., Mouritsen, H., & Dedek, K. (2023). Immunohistochemical characterization of bipolar cells in four distantly related avian species. *Journal of Comparative Neurology*, 531, 561–581. <https://doi.org/10.1002/cne.25443>